ACS OMEGA

Open Access

http://pubs.acs.org/journal/acsodf

Article

A Dual Nanoapproach for the Treatment of Depression and Sleep Via a Novel Optimized Eugenol-Mucoadhesive Nanoemulsion

Mohd Faiyaz Khan,*,∞ Niyaz Ahmad,*,∞ Khalid Ansari, Zabih Ullah, Hisham Osman Ibrahim, Hanan Mesfer Alyami, Ali Jaber Alqahtani, and Sarfaraz Ahmad

Cite This: *ACS Omega* 2025, 10, 16815−16840

Read Online

ACCESS | Metrics & More | Article Recommendations

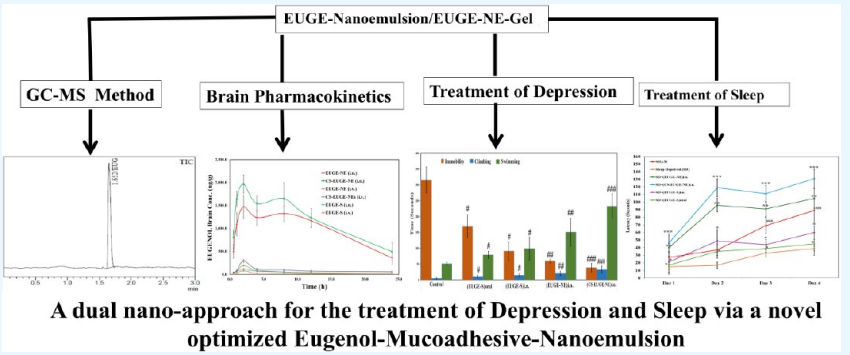

ABSTRACT: This study aimed to develop a chitosan (CHS)-coated eugenol (EUGE)-loaded nanoemulsion (CHS-EUGE-NE) to enhance brain bioavailability. A novel GC-MS/MS method was developed and validated for EUGE quantification in brain tissue and plasma alongside pharmacokinetic analysis. The nanoemulsion was optimized using a Box−Behnken design (BBD), with the final formulation containing 6.0% oil, 10% surfactant mix, and undergoing 6.5 min of ultrasonication at 30% intensity and 40 °C. The optimized CHS-EUGE-NE exhibited a globule size of 142.4 ± 11.31 nm, a polydispersity index of 0.1660 ± 0.0009, and a zeta potential of −16.20 ± 1.10 mV, which shifted to positive upon CHS coating, enhancing mucoadhesion. A linear range from 1.00 to 3000 ng/mL was established, with accuracy between 90.91% and 99.83%. Pharmacokinetic analysis demonstrated significantly increased C_{max} and AUC in the rat brain, correlated with behavioral improvements in the forced swimming test. No signs of toxicity were observed. These findings suggest that CHS-EUGE-NE is a promising nanoformulation for enhancing the brain-targeted delivery of eugenol for the treatment of depression and sleep disorders.

INTRODUCTION

Depression is a major public health concern due to its high prevalence and association with disability. According to the WHO, it is the second leading cause of illness and death after ischemic heart disease,[1] with approximately 850,000 suicide-related deaths annually.[2] Globally, depression affects 17−20% of the population, imposing a significant financial burden.[3] It manifests through psychological, behavioral, and physiological changes, including hopelessness, guilt, anhedonia, suicidal tendencies, sleep disturbances, and cognitive impairments.[4] Stress is a key contributor, with studies linking depression to hyperactivity of the hypothalamic-pituitary-adrenal (HPA) axis, which is often normalized through antidepressant treatment.[5,6]

Clove oil, extracted from *Syzygium aromaticum* (Myrtaceae), is rich in eugenol ($C_{10}H_{12}O_2$; 2-methoxy-4-(2-propenyl) phenol), a compound with analgesic and antiseptic properties. It is a pale-yellow oil, slightly soluble in water but readily dissolved in organic solvents.[7] Eugenol has shown anti-depressant-like effects in the forced swim and tail suspension tests, with oral administration (30 mg/kg) yielding results comparable to imipramine.[8,9] Several studies further support its antidepressant potential.[8−13] These findings provide strong support for further research into eugenol as a natural alternative for managing depression and related symptoms.

Sleep is essential for overall health, cognitive function, and emotional well-being. The American Academy of Sleep Medicine recommends 6−8 h of sleep per night to prevent mood disturbances, impaired concentration, and daytime sleepiness.[14−16] Approximately one-third of the global population experiences nonclinical insomnia, affecting all age

Received: January 26, 2025
Revised: March 20, 2025
Accepted: March 25, 2025
Published: April 17, 2025

groups with prevalence rates between 25% and 65%.[14−16] Chronic sleep deprivation is linked to obesity, hypertension, depression, and reduced mental and physical performance, making it a significant economic burden.[17−20] Sleep consists of REM and NREM stages regulated by neurotransmitters from the hypothalamus and reticular activating system. Increased GABA and decreased histamine levels promote NREM sleep, while treatments for insomnia target GABA, histamine, serotonin, melatonin, and orexin receptors.[21−24] Eugenol has shown anesthetic and analgesic properties, but further studies are needed to confirm its sleep-enhancing effects.[24,25] Aromatherapy using essential oils, such as clove oil, has been reported to reduce stress and depression while improving sleep quality, supporting its potential as a natural sleep aid.[26,27]

Oral drug administration can cause gastrointestinal side effects, such as nausea, vomiting, and dizziness.[28] As a result, intranasal (i.n.) drug delivery has emerged as a noninvasive alternative with improved bioavailability.[28] This method targets systemic, local, and central nervous system (CNS) effects by utilizing the olfactory and trigeminal nerve pathways to reach the brain.[29−31] However, systemic drug delivery faces limitations due to barriers like the blood-cerebrospinal fluid (BCSFB) and blood-brain barrier (BBB), hindering the effectiveness of both large and small molecules.[29] Consequently, alternative drug delivery strategies, such as intraventricular, intraparenchymal, and intrathecal methods, along with conjugation with antibodies and nose-to-brain approaches, have been explored.[32,33]

Nanoemulsions (NEs) offer high drug-encapsulation efficiency, enhancing solubility and bioavailability.[34] While "nanoemulsion" and "microemulsion" were once used interchangeably, it is now understood that microemulsions require higher surfactant concentrations (>20%) for thermodynamic stability, and their hydrodynamic diameter is smaller than that of nanoemulsions.[35,36] However, the high surfactant content in microemulsions limits their internal use, whereas nanoemulsions, requiring less surfactant, are more suitable for internal drug delivery, though they are kinetically stable. Nanoemulsion formation is not spontaneous ($\Delta G > 0$) and requires external energy for preparation.[37] In this study, the EUGE nanoemulsion was formulated by engineering oil and surfactants, followed by ultrasonication to control the droplet size. Box−Behnken and central-composite designs were used to optimize independent variables for the most effective EUGE nanoemulsion in terms of globule size, PDI, ZP, and transmittance.[38,39] Eugenol (EUGE) nanoemulsion delivered intranasally can improve brain bioavailability by increasing tissue concentrations. However, the short residence time in the nasal cavity may limit absorption.[40] To address this, incorporating mucoadhesive properties and higher viscosity can enhance the formulation's effectiveness. Mucoadhesive agents extend the contact time between the drug and nasal mucosa, improving absorption.[41,42]

Chitosan (CHS), a biodegradable polysaccharide, is widely used in protein and metal adsorption. Its surface modification of nanoparticles (NPs) enhances drug delivery by providing sustained release, improved mucoadhesion, and increased absorption. CHS coating also contributes to controlled drug release and enhanced permeation and retention due to the attraction between its positive charge and the negatively charged membrane.[28,41,42] Chitosan, recognized for its mucoadhesive properties, is widely used in protein[43,44] and metal adsorption.[45] When used in coating or encapsulating nanoemulsions, it provides benefits such as prolonged drug release and improved absorption. This study developed a mucoadhesive nanoemulsion for intranasal delivery, enhancing the absorption and retention of eugenol, which improves therapeutic effects for various conditions.[38,46]

Prior to this study, no sensitive bioanalytical methods were available for assessing eugenol's biodistribution parameters (C_{max}, T_{max}, k_e, $t_{1/2}$, AUC) in the brain, as most methods focused on food or medicinal herbs rather than eugenol alone.[47−49] This study develops the first GC-MS/MS bioanalytical method specifically for eugenol, validated according to US FDA guidelines. Our method, characterized by shorter retention times, enhanced sensitivity, and high efficiency, enables precise pharmacokinetic analysis of eugenol in both plasma and brain tissues.

This study evaluated the optimized nanoemulsion (Opt-NE) for eugenol delivery via intranasal administration to the brain. We compared CHS-EUGE-NE, EUGE-NE, and EUGE-S formulations for their effects on depression, sleep-related issues, and pharmacokinetic parameters using a novel, sensitive GC-MS/MS bioanalytical method in rats. Intranasal administration of CHS-EUGE-NE improved the brain bioavailability of eugenol and reduced side effects. This research is the first to use chitosan-coated EUGE-NE, demonstrating significant therapeutic effects on depressive symptoms and sleep deprivation, along with a comprehensive analysis of in vivo and in vitro parameters.

MATERIALS AND METHODS

Materials. Eugenol was procured from Santa Cruz Biotechnology (USA), and Chitosan (molecular weight 50,000−190,000 Da, degree of deacetylation 75−85%) was purchased from Sigma-Aldrich Chemicals Co., St. Louis, MO, USA. Clove oil, Transcutol-HP (Gattefossé, France), Tween 20, and other surfactants were sourced from Sigma Life Science, Sigma-Aldrich (Belgium). LC-MS-grade solvents, such as ethanol, acetonitrile, and methanol, were obtained from Fluka, Sigma-Aldrich. All materials used in this study had a purity of 99.9%. Milli-Q water was utilized, and other analytical-grade reagents and chemicals were acquired from various commercial suppliers.

Development of Nanoemulsion. *Screening of Excipients for Development of Novel Nanoemulsion.* Before developing the nanoemulsion, it was essential to choose the right surfactants and oil. Each and all excipients were chosen based on their ability to dissolve the drug and their stability for creating the novel nanoemulsion. The solubility of eugenol was tested with various oils, including clove, sesame, almond, eucalyptus, castor, peanut, oleic acid, soybean, and Lauroglycol FCC. The oils selected were readily available and demonstrated no biodegradability.[38] We also conducted solubility assessments on various surfactants, including Pluronic F-68, Tween 20, Carbitol, Maisine, Transcutol HP, Tween 80, ethanol, and PEG-400.

In summary, a solubility study was conducted in which a maximum quantity of eugenol was placed in an MCT, i.e., a microcentrifuge tube that had 1 mL of solvent (such as oil or surfactant). The mixture was vortexed for up to 72 h at room temperature using a cyclomixer. After this period, excess eugenol was removed through centrifugation (KUBOTA Centrifuge) at rpm (3000) for 10 min. Subsequently, the supernatant (10 μL) was shifted to fresh MCT, and the volume was adjusted to with methanol (1 mL). After vortexing, the

https://doi.org/10.1021/acsomega.5c00783
ACS Omega 2025, 10, 16815−16840

mixture was filtered using a nylon filter made up of nylon (0.22-μm). The absorbance was measured at a wavelength of 281 nm following the appropriate dilutions. The amount of eugenol solubilized in the selected oil, surfactant, or cosurfactant was determined using a previously established calibration curve.[38] Following the solubility assessment, we initiated an excipient screening study by evaluating the optimized-NE stability.

Pseudoternary Phase Diagram (PTPD) Creation. In constructing the pseudoternary phase diagram, three axes were established: one for the oil phase, another for the aqueous phase, and the third for the ratio of surfactants (Smix). The surfactant ratio was optimized using the PTPD method, which allowed us to identify the largest area corresponding to the oil-in-water (o/w) nanoemulsion region. Clove oil was chosen as the oil phase, Tween 80 was selected as the surfactant, and PEG 400 was used as the cosurfactant based on the results of the aqueous phase titration method performed. The oil was mixed with the surfactant and cosurfactant (S_{mix}) and subsequently titrated with distilled water to create the nanoemulsion. Various S_{mix} ratios were tested to optimize the surfactant concentration including 5:1, 4:1, 3:1, 2:1, 1:3, 1:2, 1:1, and 1:0. Additionally, numerous nanoemulsion regions were identified through 16 trials with different oil and Smix ratios, such as 1:9, 3:7, 1:2.3, 2:8, 1:4, 5:5, 1:1, 4:6, 1:1.5, 7:3, 1:0.43, 6:4, 1:0.7, 8:2, 1:0.25, 1:8, 1:2, 1:3.5, 1:8, 1:5, 1:7, 1:6, 9:1, 1:0.1, and 1:3. During the development of the PTPD, each titration step was closely observed for changes in turbidity and clarity.[38]

Design and Development of EUGE-Loaded Nanoemulsion. To optimize the Eugenol Nanoemulsion (EUGE-NE), a BBD (i.e., Box–Behnken Design Software) was employed, involving five factors at four levels. The optimization process included the following independent variables: Clove Oil as the oil phase: X_1, a 3:1 ratio of Tween-80 (surfactant) to cosurfactant: PEG 400: X_2, ultrasonication time (in minutes) (X_3), ultrasonication intensity (in %) (X_4), and temperature (°C) (X_5). A total of forty-six experimental runs were conducted, each varying in independent variable levels, categorized as low, medium, and high (refer to Table 1). The dependent responses measured included Y_4 = Zeta Potential (mV), Y_2 = Transmittance (%), Y_1 = Globule Size (nm), and Y_3 = Polydispersity Index (PDI). Additionally, 3D response surface plots were generated to visualize the impact of the independent variables on the measured responses. The responses from each run were analyzed using linear, 2F1, cubic, and quadratic models to identify the best-fitting model. The software generated contours and 3D plots to evaluate the influence of each independent factor on the respective responses. The actual values for every response were compared quantitatively with the predicted values generated by BBD. A normal polynomial equation was derived for the quadratic model from the Box–Behnken design (BBD) to evaluate the impact of the independent variables on the responses, as detailed below (eq 1):

$$Y = b_0 + b_1A + b_2B + b_3C + b_{12}AB + b_{13}AC + b_{23}BC + b_{11}A^2 + b_{22}B^2 + b_{33}C^2 + \ldots \quad (1)$$

In this context, Y represents the response variable with b_0 serving as the intercept. The coefficients b_1, b_2, and b_3 are linear coefficients, and b_{11}, b_{22}, and b_{33} indicate the squared coefficients associated with the quadratic terms. Additionally, b_{12}, b_{13}, and b_{23} are the interaction coefficients that reflect the combined effects of two variables.[39,50]

Table 1. Variables in "Design Expert" Software for Preparation and Optimization of Eugenol Nanoemulsions (EUGE-NE)

Independent variables	Levels		
	Low (−1)	Medium	High (+1)
X_1 = Oil (% v/v)	2.0	6.00	10.0
X_2 = Smix (% v/v)	10	15.00	20
X_3 = Ultrasonication time (minutes)	3	6.50	10
X_4 = Ultrasonication intensity (%)	20	35.00	50
X_5 = Temperature (°C)	20	32.50	45
	Constraints	Importance	
Independent variables			
X_1 = Oil (% v/v)	In range	− − − − −	
X_2 = Smix (% v/v)	Minimize	+ + + +	
X_3 = Ultrasonication time (min.)	In range	− − − − −	
X_4 = Ultrasonication intensity (%)	Minimize	+ + + + +	
X_5 = Temperature (°C)	In range	− − − − −	
Dependent variables			
Y_1 = Globule Size (nm)	Minimize	+ + + + +	
Y_2 = Transmittance (%)	Maximize	+ + + + + + +	
Y_3 = Polydispersity Index (PDI)	Maximize	+ + + +	
Y_4 = Zeta Potential (mV)	Minimize	+ + + +	

Formulation and Development of Eugenol-Loaded Nanoemulsion (NE). Eugenol-loaded nanoemulsion was formulated with the help of a high-energy ultrasonication method. Eugenol was dissolved in clove oil in a glass vial according to the required oil quantity. Then, a surfactant mixture (Smix) was added. The resulting mixture was microtitrated with distilled water to create a coarse emulsion. Ultrasonication was applied at amplitude (30%) for 6.5 min to transform the coarse emulsion into a nanoemulsion, utilizing an ultrasonic processor (Fisher Scientific Technology, USA).[39] The application of high-energy ultrasonication led to heat generation due to the cavitation effect. To minimize excessive heat, the sonication was performed in short intervals. If overheating occurred, a sample container was kept in a properly sealed ice bath to control the temperature.[51,52] The optimized nanoemulsion demonstrated a globule size of less than 100 nm. This was attributed to the dominant influence of Brownian motion, which contributed to the kinetic stability of the nanoformulation, ensuring its stability over extended storage periods.[51,52]

Characterization of Optimized Eugenol-Loaded Nanoemulsion. *% Transmittance, Analysis of Globular Size, ZP, and PDI Determination.* The nanoemulsion's reduced globule size led to an increase in surface area, enhancing drug absorption when incorporated into the nanoemulsion. Therefore, globule size is a crucial parameter in nanoemulsion formulations.[38] The globule size, zeta potential, and PDI of the formulation were analyzed by using a Malvern Zetasizer Nano ZS (UK). The formulation was diluted 50 times prior to the size measurement. The analysis was conducted at a temperature of 25.0 ± 1.0 °C, with light scattering measured at a 90° angle.[39]

UV–Vis Spectrophotometry Analysis. A Shimadzu UV–vis spectrophotometer (Japan) was used to measure the % transmittance of the optimized Eugenol-loaded nanoemulsion. The nanoemulsion was analyzed without dilution, using Milli-Q water as the blank.[51]

https://doi.org/10.1021/acsomega.5c00783
ACS Omega 2025, 10, 16815−16840

Transmission Electron Microscopy (TEM) Analysis. The size, shape, and structure of the formulated nanoemulsions (NEs) were examined using TEM (FEI Morgagni 268 at 80 kV). A sample of the NEs was kept on TEM grids, which were coated with a carbon support film featuring holes. After being air-dried, the grids were inserted into the imaging from TEM. A representative image was captured.[52]

Viscosity, Refractive Index, and pH Measurement. The pH of the opt-NE was examined using a pH meter (EUTECH Instruments, Singapore), while the refractive index was determined using an Abbe-type refractometer. Conductivity was assessed using a conductivity meter with platinized electrodes, by passing an electric current through 20.0 mL of the opt-NE. Viscosity was measured without dilution using a Brookfield viscometer (A& D Instruments Viscometer SV-10, Japan). The whole experiments were performed at room temperature (25 ± 1.0 °C).

Preparation of Mucoadhesive Eugenol-Loaded Nanoemulsion (CHS-EUGE-NE). The previously mentioned method was used to prepare the optimized eugenol-loaded nanoemulsion (EUGE-NE). A chitosan (CHS: 1%w/v) solution was gradually added drop by drop to the Eugenol-NE while continuously stirring for 10 min. This procedure led to the creation of a clear and transparent mucoadhesive Eugenol nanoemulsion based on CHS (CHS-Eugenol-NE).[42]

In Vitro Release Study of Eugenol. An *in vitro* release study was conducted using a dissolution apparatus to examine the release of Eugenol from the optimized Eugenol-loaded nanoemulsion (Opt-Eugenol-NE) and CHS-Eugenol NE. Samples (2 mL each) were placed separately in dialysis bags, which were carefully sealed to prevent leakage. At specified time intervals, 5 mL samples were collected, with an equivalent volume of fresh buffer added to maintain the total volume for subsequent analysis. The release rate of Eugenol was determined using GC-MS/MS analysis. The release data were fitted to various models, including Higuchi-, Korsmeyer−Peppas-, first-order-, and zero-order models.[38]

Ex Vivo Eugenol Permeation Study for Optimized Nanoemulsion. Nasal tissues were freshly and carefully obtained from the nasal cavities of goats at a resident slaughterhouse. A fixed area of 0.785 cm^2 was utilized for the permeation study of Eugenol using a Logan Instrument Corporation setup (Piscataway, NJ, USA). The receptor chamber was filled with phosphate-buffered saline (20 mL) at 7.4 pH and maintained at 37 °C. After a preincubation period of 20 min, Eugenol nanoemulsion (NE) and CHS-Eugenol-NE were introduced into the donor chamber. At each designated time interval, samples (1 mL) were taken from the receptor chamber. Each sample was passed through a membrane filter for quantification. The permeation of Eugenol into the nasal tissues was assessed using a developed GC-MS/MS method.[41]

Stability Study of Eugenol Nanoemulsion Under Different Storage Conditions. Unlike microemulsions, which are kinetically stable, nanoemulsions are not thermodynamically stable and can experience stability issues such as coalescence or Ostwald ripening. Therefore, it is essential to evaluate the stability profile of the optimized Eugenol nanoemulsion. The stability of Opt-Eugenol-NE was assessed over a period of 14 weeks at room temperature, i.e., 25 ± 1 °C. To investigate stability (long-term), the nanoemulsion was evaluated under two conditions: one subjected to sonication (Opt-Eugenol-NE) and the other without sonication (Eugenol-NEW). The primary parameter for stability testing was the globule size. Changes in globule size were monitored at various intervals throughout the storage study, specifically at 0, 2, 4, 6, 8, 12, and 14 weeks.[38]

In Vivo Study. Ethical approval for the study (BERC-009-04-23) was obtained from the Bioethical Research Committee (BERC) at Prince Sattam bin Abdulaziz University for pharmacokinetic (PK) and pharmacodynamic (PD) research. The care and handling of the animals adhered to internationally recognized guidelines for animal research. All experiments were conducted in accordance with the standards set by the Institute of Laboratory Animal Resources, Commission on Life Sciences, National Research Council (1996). The study utilized rats weighing between 200 and 300 g, with housed in each cage (3 rats). The animals were maintained under a natural light and dark cycle, ensuring they had continuous access to food and water in a controlled environment at 20−30 °C and 50−55% humidity. The study was carried out under standard conditions for the laboratory, and experiments were conducted throughout the light cycle when the animals were awake.

Bioanalytical Method Development and Validation. The bioanalytical method for detecting Eugenol in brain homogenate and plasma was developed and validated in accordance with U.S. FDA guidelines.[67] Eight various concentrations were prepared and chosen to create a calibration curve (CC), which was established based on the peak area ratio and a $1/x^2$ weighted linear least-squares regression.[28,67] To assess the signal-to-noise ratio (10:1) for quantifying Eugenol after extraction, several quality control samples were prepared, including the LLOQ, as well as lower (LQC), medium (MQC), and higher (HQC) quality controls. Six prespiked-extracted samples, i.e., mean area response were compared with postextraction-spiked samples that were free of Eugenol in various matrices. For each quality control level (LLOQ, LQC, MQC, and HQC), six separately prepared samples were selected, along with one complete calibration curve sample from each matrix (e.g., plasma as well as brain homogenate) to examine inter- and intraday precision and accuracy.

Parameters for GC-MS/MS Analysis. The quantification of Eugenol was performed using a highly sensitive GC-MS system, specifically the Shimadzu TQ8040 NX with an autosampler. The stationary phase for the VF-5 ms column (40 m × 0.25 mm i.d. × 0.25 μm) is made of 5% phenyl, 95% dimethylpolysiloxane (Agilent Technologies, USA) with an injection volume of 1 μL and a total run time of 3 min. Helium served as the carrier gas, with 1 mL/min steady flow rate. The temperature of the GC oven was set to increase from 40 °C (held for 1 min) to 220 °C (held for 1 min) at a rate of 5 °C/min. The injection was performed in split mode (10:1) at a temperature of 240 °C. The mass detector utilized was GC-MS Shimadzu TQ8040 NX, known for its high sensitivity and resolution. The mass transitions m/z 164.10 and 149.10 were used for the quantification of Eugenol. The Lab Solution Software (Kyoto, Japan) was employed to analyze the amount of Eugenol.

Preparation of Samples for Quality Control and CC. A Eugenol stock solution was made in ethanol (1-mg/mL). Eight different aqueous dilutions were prepared from the stock solution for the CC, with 2%-Eugenol added to each in various blank matrices, including plasma and animal brain homogenate. The spiking was performed by mixing 20 mL of aqueous Eugenol with 980 mL of the respective blank matrix. The eight

https://doi.org/10.1021/acsomega.5c00783
ACS Omega 2025, 10, 16815−16840

different concentrations of the Eugenol drug, ranging from 1.0 to 3000 ng/mL, included 1.0, 2.0, 40.0, 650.0, 1275.0, 1920.0, 2550.0, and 3000.0 ng/mL. A similar preparation method was used for the quality control samples, which included concentrations of HQC (2400 ng mL^{-1}), MQC (1250 ng mL^{-1}), LQC (2.92 ng mL^{-1}), and LLOQC (1.01 ng mL^{-1}). The spiked dilutions were prepared fresh and kept at a temperature ranging from 2 to 8 °C.

Bioanalytical Extraction. The samples for the quality control (QC) and calibration curve (CC) were freshly made using unknown samples of brain homogenate or plasma for analysis. An aliquot of 215 μL was moved to a clean glass tube for matrix extraction, and then 175 μL of 5% formic acid was added. The mixture was vortexed (at 300 rpm) for 6 min to break down the matrix proteins. The samples were subsequently centrifuged (4000 rpm) at 4 °C (10 min) to separate the phases, followed by a 7 min settling period for any residues. The supernatant (2.5 mL) was cautiously collected using a pipet and transferred to a new glass tube. To facilitate evaporation, the samples were placed in a water bath (37 °C) under a stream of nitrogen gas until dry. The residues in the dried test tubes were rehydrated with mobile phase (750 μL) and mixed using a vortex mixer at 300 rpm (2.5 min). These samples were then placed in GC-MS vials for quantification. Specifically, 550 μL from each prepared sample was mixed with acetonitrile (300 μL) to precipitate proteins, then vortexed (300 rpm, 5 min). The samples were centrifuged (4000 rpm) for 12 min, and the supernatant (250 μL) was placed into GC-MS injection vials. For GC-MS analysis, 150 μL of acetonitrile was added to each vial, followed by vortexing, and the reaction was allowed to proceed at room temperature for 15 min. Finally, the vials were positioned in an autosampler for bioanalytical analysis.

Pharmacokinetic Evaluation (PK). In this pharmacokinetic evaluation, we established six groups: Group I (G-I) received EUGE-S (intranasally), Group II (G-II) received EUGE-S (intravenously), Group III (G-III) received EUGE-NE (intranasally), Group IV (G-IV) received EUGE-NE (intravenously), Group V (G-V) received CHS- EUGE-NE (intranasally), and Group VI (G-VI) received CHS- EUGE-NE (intravenously). Each animal received a dose based on b. wt. (10 mg kg^{-1}) of Eugenol. For each sampling time point, three animals from each group were examined. Blood samples were obtained from each animal, and following euthanasia, lung and brain tissues were collected to make the homogenates. All matrices were extracted according to the method described in the section of Bioanalytical Extraction for pharmacokinetic evaluation. Samples were collected at specific time intervals: 0.0, 0.50, 1.0, 2.0, 4.0, 8.0, 12.0, and 24.0 h. The collected samples were processed as outlined earlier and analyzed using our lab's bioanalytical method to determine parameters like $t_{1/2}$, elimination rate constant (k_e), maximum concentration (C_{max}), and area under the curve (AUC_{0-t}). A total of 24 animals were allocated for each group (8 animals per group), resulting in a total of 144 animals across the six groups. Blood collection and tissue sampling were conducted as described above, and all homogenate samples were made and examined using the previously described GC-MS/MS method.[38]

Pharmacodynamic Evaluation: Behavioral Analysis. A behavioral analysis was conducted to assess the antidepressant effects of Eugenol. This investigation serves as a crucial method for understanding the impact of neurotransmitter function in the brain of the animals. The forced swim test (FST) and locomotor activity test were utilized to compare the antidepressant effects of the various formulations of opt-EUGE.[53] The forced swim test (FST) is a simple, rapid, and cost-effective method widely employed to assess the antidepressant effects of drugs. This test is based on the principle of inducing immobility, which helps to evaluate depressive behaviors. Stress can lead to reduced muscle movement, accompanied by alterations in neurochemistry, resulting in signs similar to depression. Additionally, locomotor activity assessments are utilized to further determine the antidepressant effects of various substances.[54,55]

Experimental Design for the Depression Study. We established six groups to assess the effects of various treatments on depression in animals during pharmacodynamic evaluation. Group I: control group with untreated rats. Group II: EUGE-S (oral) at a dosage of 10 mg kg^{-1} bd. wt. Group 3: EUGE-S (Eugenol) was administered intranasally at 10 mg kg^{-1} bd. wt. Group 4: received the Eugenol-loaded nanoemulsion (EUGE-NE) intranasally at the same dosage of 10 mg kg^{-1} bd. wt. Finally, Group V was treated with the mucoadhesive Eugenol-loaded optimized nanoemulsion (CHS-EUGE-NE) intranasally, also at 10 mg/kg body weight. An oral dose was delivered using a syringe fitted with a 16-gauge ball-tipped feeding needle. The rats were positioned at a slight incline at the time of intranasal administration of the different optimized nanoemulsions. The formulations were administered into both nostrils using a micropipette made from polyethylene, targeting the nasal cavity (posterior part). Behavioral studies were conducted using the forced swim test (FST) and locomotor activity assessments.

Forced Swim Analysis. A glass tank that is made of cylindrical shape measuring 46 cm in height and 20 cm in diameter was kept with fresh water to a depth of 30 cm, into which the animals from each group were placed. The activities of climbing, swimming, and immobility were recorded and analyzed to assess the average effects of all treatments following administration.[38,54,55] The duration of the climbing was recorded when the rats vigorously ascended the walls of the tank. Conversely, periods during which the rats floated and exhibited minimal movement were documented as the immobility time. Active swimming was noted and recorded as swimming time.[38,53] The mean values for swimming, climbing, and immobility were calculated to evaluate the effectiveness of the treatment for depression.[55] When a rat decreased its movements while floating, this was noted as immobility. Conversely, if the rats actively used their forepaws to move along the sides of the tank, then this was documented as climbing. Active swimming within the tank was noted as the swimming duration.

Photoactometer Examination. A digital photoactometer, equipped with infrared-sensitive photocells, was utilized to assess the locomotion of rats, commonly referred to as the photoactometer examination, i.e., locomotor activity test or LAT. The animals were acclimated to the photoactometer chamber, i.e., 30 × 30 cm^2 for a duration of 15 days. Once kept in the chamber, 6 red light beams were activated, positioned 2 cm above floor, and oriented in opposite directions. The interruption of each beam was recorded on the display screen.[38,53] When the light beams were interrupted, the time for recording locomotor activity (LAT) commenced. The count was taken for each rat that crossed in front of the light beam and calculated over a period of 5 min. Only a rat was

https://doi.org/10.1021/acsomega.5c00783
ACS Omega 2025, 10, 16815−16840

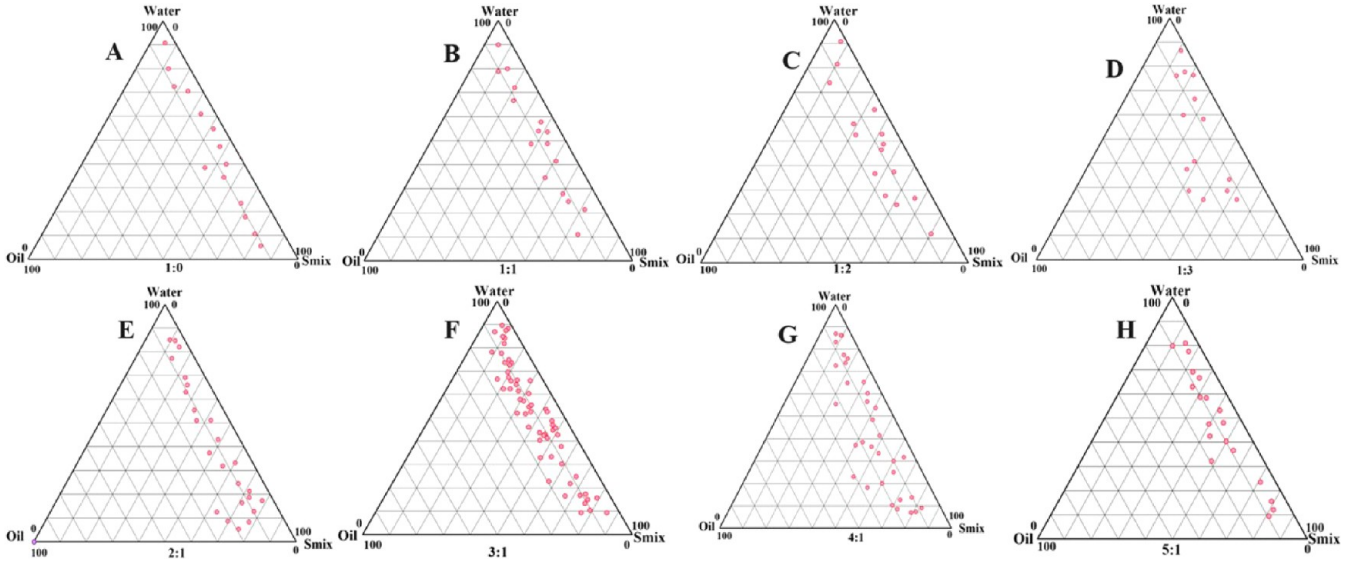

Figure 1. Phase diagrams developed by the aqueous phase titration method for EUGE-NE Eugenol zones (as dotted area) for Eugenol used as Oil Phase, Tween-80, PEG 400, and Milli-Q-water at Smix ratios of A = 1:0, B = 1:1, C = 1:2, D = 1:3, E = 2:1, F = 3:1, G = 4:1, and H = 5:1.

tested at a time within the chamber to assess its movement, allowing for accurate measurement of LAT. Different groups of animals received the optimized preparations separately to facilitate a comparison of LAT activity.

Sleep Deprivation (SD). Earlier research involving animal models has shown the biological impacts of different homeopathic treatments for sleep deprivation (SD).[56,57] Nunes et al. employed the multiple platform method (MPM) as an animal model to induce sleep deprivation.[58] This method has been utilized in numerous studies[59−61] and has demonstrated effectiveness in inducing rapid-eye-movement, i.e., REM deprivation in rats, resulting in lower stress levels compared to other established sleep deprivation techniques.[62,63]

Rats were randomly divided into six groups: SHAM, sleep deprived (SD), SD+(EUGE-NE)i.n., SD+(CHS-EUGE-NE)i.n., SD+(EUGE-S)i.n., and SD+(EUGE-S)oral. Beginning on postnatal day (PND) 70, the rats underwent sleep deprivation for 48 h using the multiple platform method (MPM) described below.[60] A placebo was administered orally starting one h after the baseline tests (1 h post-SD) and continued every three h during the subsequent 24 h. One hour after SD and before treatment, the rats were assessed in the startle box to obtain baseline measurements. Furthermore, assessments were conducted at 6, 12, and 24 hours, as well as 14 days post-SD. Prepulse inhibition (PPI) was measured at 12 and 24 hours, while a motor-learning test on the rotor rod was conducted starting 48 h post-SD and continued for a total of four-days training. The rats were acclimated before any experimental procedures.

Multiple Platform Method (MPM). The multiple platform method (MPM) utilizes the characteristic muscle atonia associated with REM sleep. In brief, this technique, adapted from previous studies,[60] entails positioning the animal on a narrow platform located inside a water tank. When the animal relaxes and experiences muscle atonia, it falls into the water, resulting in deprivation of REM sleep.

In this study, a water tank with a diameter of 120 cm and a height of 60 cm was utilized, containing 30 narrow platforms, each measuring in diameter (6.50 cm). Sixteen rats were kept on the platforms during each session, permitting them to freely move. The tank was occupied with water to a distance (6 cm), keeping it below (1 cm) the platform to allow the rats to climb back out if they fell in. The exposure to the multiple platform method (MPM) commenced at 08:00 and lasted for 48 h. To assess the efficiency of the MPM, the rats were recorded using an infrared Ikegami camera. The room temperature was kept constant at 23 ± 1 °C, and the animals had unlimited access to food and water. All rats successfully completed the study without any fatalities.

Rotor-Rod Test for Sleep. The rotor-rod apparatus (San Diego Instruments, San Diego, CA, USA) is designed to evaluate coordination, motor functions, learning, and balance. Constructed from black, nonreflective Perspex, it features a rotating rod divided into 4 lanes via impervious black barriers. A sawdust-filled area (45.70 cm high) is included for safe landings, and the system automatically records latencies in seconds using red-beams. Every learning session contains 4 trials conducted over four consecutive days. On the first day, rats are given a 30 s acclimatization period in the apparatus. Each trial begins at a speed of 5.0 rpm and lasts for 15 s, with a constant acceleration of 0.1 rpm/second, reaching a 50 rpm highest speed after 7.5 min.[60]

Toxicological Evaluation of Optimized Nanoemulsion. A toxicity estimation was conducted on CHS-NE without Eugenol (Gr-E: brain, Gr-B: nasal mucosa of rat) and CHS-EUGE-NE (Gr-F: brain, Gr-C: nasal mucosa of rat) to assess the histological effects on the brain and nasal mucosa at a dose of 10 mg/kg of Eugenol. The dose was administered intranasally between 9:00 and 10:00 a.m. daily for 14 days. The animals were monitored daily for any signs of morbidity, mortality, or abnormal behavior. The normal control groups were Gr-A and Gr-D for the brain and nasal mucosa of rat, respectively. At the end of the 14-day period, the rats were sacrificed to collect brain and nasal mucosa samples for histological analysis. Tissue sections were prepared using a 10% neutral-buffered formalin solution and stained with eosin and hematoxylin to inspect any histological changes compared to the standard group.

https://doi.org/10.1021/acsomega.5c00783
ACS Omega 2025, 10, 16815−16840

Statistical Examination. Results will be expressed as mean ± SEM. Statistical evaluations will be conducted with the help of Student's *t*-test to assess differences, along with ANOVA to analyze the p-values. ANOVA is utilized to determine the differences among population means by comparing the variation within each sample to the difference between the samples.

RESULTS AND DISCUSSION

Nanoemulsion Optimization. Eugenol was mixed with the chosen oil (such as clove oil) in the necessary amounts. If a drug is not dissolved properly, it can lead to precipitation, resulting in an unstable nanoemulsion during its shelf life.[38] Clove oil demonstrated the highest solubility for eugenol, making it the preferred oil phase. Tween 80 was found to have excellent solubility compared with other surfactants and was also compatible with clove oil. As a result, Tween 80 was chosen as the surfactant. PEG 400 was chosen as the cosurfactant due to its high solubility and compatibility with both clove oil and Tween 80.

The pseudoternary phase diagram was employed to assess the maximum isotropic nanoemulsion (NE) region for the selection of the Smix (surfactant and cosurfactant mixture) ratio. As shown in Figure 1, increasing the amount of surfactants improved the emulsification, expanding the NE region as the Smix ratio enhanced from 1:0 to 3:1.[64] However, further increasing the Smix ratio to 4:1 led to a reduction in the NE region, indicating that an excessive amount of surfactant does not necessarily enhance the emulsification. Based on these findings, a 3:1 Smix ratio was selected for the formulation of Eugenol-NE. The selected Smix ratio had a hydrophilic−lipophilic balance (HLB) value of 11.83, which indicated satisfactory conditions for forming an o/w nanoemulsion.[42] The observed responses, including globule size, polydispersity index, zeta potential, and percentage transmittance, closely aligned with the predicted responses.[39,64]

Optimization of EUG Nanoemulsion by Using BBD. The optimization of the Eugenol Nanoemulsion (EUGE-NE) was conducted using the Box−Behnken design. The current study focused on enhancing the development of EUGE-NE through the ultrasonication technique by varying the various percentages of the oil phase (clove oil), the surfactant and cosurfactant mixture (the ratio of S_{mix}, including Tween-80 and PEG 400), and the duration of ultrasonication. The dependent variables assessed were globule size (nm) (Y_1), %transmittance (Y_2), polydispersity index (Y_3), and zeta potential (mV) (Y_4) of the formulated Eugenol nanoemulsion (EUGE-NE) (Table 2). The independent variables were selected on the basis of preliminary experimental results.

The optimization yielded globule size (42.4 nm), transmittance (93.6%), PDI (0.166), and ZP (−19.7 mV) (Table 2). The quadratic model was identified as being the most suitable fit for all responses, with globule size, transmittance, PDI, and zeta potential, as shown in Tables 2−5. The quadratic model exhibited a higher R^2 value compared to other models (refer to Tables 3 and 4). The following are the polynomial (i.e., quadratic) equations for every individual response generated by the software:

$$Y_1 = 384.87 + 27.07X_1 + 30.46X_2 - 7.16X_3 + 22.02X_4 - 39.26X_5 + 0.00X_1X_2 + 25.0X_1X_3 + 0.00X_1X_4 + 0.00X_1X_5 - 25.00X_2X_3 - 15.28X_2X_4 + 97.60X_2X_5 + 0.00X_3X_4 + 0.00X_3X_5 + 34.17X_4X_5 - 26.89X_1^2 - 65.54X_2^2 - 35.23X_3^2 - 28.59X_4^2 - 55.76X_5^2 \quad (2)$$

$$Y_2 = 77.31 - 1.08X_1 - 3.04X_2 + 1.32X_3 - 1.58X_4 + 2.04X_5 - 0.5075X_1X_2 + 0.71X_1X_3 + 0.62X_1X_4 - 0.2425X_1X_5 - 0.47X_2X_3 + 1.74X_2X_4 - 7.36X_2X_5 - 0.79X_3X_4 - 2.39X_3X_5 - 0.04X_4X_5 - 2.33X_1^2 + 3.86X_2^2 - 2.01X_3^2 - 2.82X_4^2 + 2.07X_5^2 \quad (3)$$

$$Y_3 = +0.52 + 0.0132X_1 + 0.035X_2 + 0.0201X_3 + 0.0345X_4 - 0.0387X_5 + 0.0093X_1X_2 - 0.0835X_1X_3 - 0.01225X_1X_4 + 0.0322X_1X_5 + 0.048X_2X_3 - 0.021X_2X_4 + 0.1124X_2X_5 + 0.0965X_3X_4 + 0.0255X_3X_5 + 0.0103X_4X_5 - 0.0519X_1^2 - 0.12X_2^2 - 0.1019X_3^2 - 0.0120X_4^2 - 0.12X_5^2 \quad (4)$$

$$Y_4 = -21.20 - 2.12X_1 - 1.22X_2 - 1.79X_3 - 0.72X_4 - 0.16X_5 - 0.12X_1X_2 - 0.125X_1X_3 - 0.12X_1X_4 + 1.1025X_1X_5 - 0.12X_2X_3 - 0.059X_2X_4 + 0.379 \times X_2X_5 - 0.1175X_3X_4 - 1.55X_3X_5 - 0.25X_4X_5 + 2.74X_1^2 + 0.423X_2^2 + 5.24X_3^2 + 2.48X_4^2 + 2.62X_5^2 \quad (5)$$

where $A(X_1)$, $B(X_2)$, $C(X_3)$, $D(X_4)$, and $E(X_5)$ represent the coded values for Clove Oil (oil phase), the Smix ratio of Tween-80 (surfactant) and PEG 400 (cosurfactant), ultrasonication time (in minutes), ultrasonication intensity (in %), and temperature (in °C), respectively. A positive sign indicates a beneficial effect, whereas a negative sign indicates a detrimental effect on the dependent variables or responses. The lack of fit for entire responses was found to be nonsignificant, i.e., $p > 0.05$ (95% confidence interval). Additionally, the other parameters of the quadratic model were deemed significant, i.e., $p < 0.0001$, demonstrating maximum values of F and a value of "Adequate Precision" which is greater than 3. This indicates that the model accurately represents the data and delivers a dependable signal.

Impact of Independent Variables on Globule Size. The size of globules in EUGE-NEs was observed to range from 142.4 to 385.83 nm. The impact of the independent variables on globule size is illustrated through polynomial eq 2, along with 3D and contour plots (Figure 2). The oil phase exhibited a positive correlation with the size of the nanoemulsion globules. Specifically, as the percentage of oil increased from 2.0% to 10.0%, the size of the globules also increased. This growth in size can be attributed to the aggregation of particles. The second variable, Smix, also positively influenced the globule size. An increase in concentration from 10.0% to 20.0%

https://doi.org/10.1021/acsomega.5c00783
ACS Omega 2025, 10, 16815−16840

Table 2. Nanoemulsion Trials Were Done Through "Design Expert" Software at Independent Variables and Their Responses

	Independent variables					Dependent variables							
	Coded factors					Observed responses				Predicted responses			
Formulation code	X_1	X_2	X_3	X_4	X_5	Y_1	Y_2	Y_3	Y_4	Y_1	Y_2	Y_3	Y_4
EUGE-NE1	2	10	6.5	35	32.5	238.93 ± 19.21	82.30 ± 3.10	0.3126 ± 0.0007	-14.58 ± 0.18	234.91	82.45	0.3094	−14.82
EUGE-NE2	10	10	6.5	35	32.5	293.07 ± 21.01	81.15 ± 1.98	0.3205 ± 0.0006	-18.59 ± 0.19	289.05	81.30	0.3173	−18.83
EUGE-NE3	2	20	6.5	35	32.5	295.31 ± 20.84	77.25 ± 1.36	0.3631 ± 0.0008	-17.04 ± 0.17	295.83	77.38	0.3603	−17.01
EUGE-NE4	10	20	6.5	35	32.5	349.45 ± 23.53	74.07 ± 1.62	0.408 ± 0.0009	-21.53 ± 0.13	349.97	74.20	0.4052	−21.50
EUGE-NE5	6	15	3	20	32.5	305.58 ± 22.14	72.07 ± 1.43	0.4454 ± 0.0010	-11.12 ± 0.08	306.2	71.95	0.4479	−11.08
EUGE-NE6	6	15	10	20	32.5	291.25 ± 18.06	76.29 ± 2.19	0.2926 ± 0.0008	-14.47 ± 0.10	291.87	76.17	0.2952	−14.43
EUGE-NE7	6	15	3	50	32.5	348.71 ± 22.46	70.51 ± 1.69	0.3211 ± 0.0007	-12.37 ± 0.11	350.24	70.38	0.3239	−12.28
EUGE-NE8	6	15	10	50	32.5	334.38 ± 21.94	71.57 ± 1.89	0.5543 ± 0.0008	-16.19 ± 0.12	335.91	71.44	0.5572	−16.10
EUGE-NE9	6	10	6.5	35	20	367.24 ± 20.73	77.07 ± 2.37	0.4008 ± 0.0006	-16.58 ± 0.16	369.98	76.89	0.4046	−16.41
EUGE-NE10	6	20	6.5	35	20	242.22 ± 17.36	85.04 ± 3.14	0.2595 ± 0.0004	-19.21 ± 0.23	235.69	85.52	0.2493	−19.60
EUGE-NE11	6	10	6.5	30	40	142.4 ± 11.31	93.60 ± 5.33	0.1660 ± 0.0009	−19.70 ± 0.052	149.23	91.40	0.1712	−19.80
EUGE-NE12	6	20	6.5	35	45	348.54 ± 23.05	75.53 ± 2.63	0.3827 ± 0.0007	-19.38 ± 0.35	352.37	74.87	0.3966	−19.15
EUGE-NE13	2	15	3	35	32.5	326.57 ± 21.83	73.60 ± 2.86	0.2459 ± 0.0003	-9.51 ± 0.26	327.84	73.44	0.2493	−9.43
EUGE-NE14	10	15	3	35	32.5	330.71 ± 22.57	70.02 ± 2.72	0.4393 ± 0.0007	-13.51 ± 0.19	331.98	69.85	0.4427	−13.43
EUGE-NE15	2	15	10	35	32.5	262.24 ± 18.41	74.82 ± 2.79	0.4531 ± 0.0010	-12.84 ± 0.21	263.51	74.66	0.4566	−12.77
EUGE-NE16	10	15	10	35	32.5	366.38 ± 20.51	74.08 ± 2.61	0.3125 ± 0.0009	-17.34 ± 0.26	367.65	73.91	0.3160	−17.26
EUGE-NE17	6	15	6.5	20	20	350.36 ± 20.19	76.23 ± 2.83	0.4071 ± 0.0006	-15.56 ± 0.24	351.93	76.06	0.4107	−15.47
EUGE-NE18	6	15	6.5	50	20	327.34 ± 19.82	73.06 ± 2.98	0.4577 ± 0.0012	-16.45 ± 0.25	327.64	72.99	0.4591	−16.43
EUGE-NE19	6	15	6.5	20	45	209.14 ± 16.08	79.78 ± 2.69	0.3218 ± 0.0011	-15.06 ± 0.28	205.07	80.22	0.3127	−15.30
EUGE-NE20	6	15	6.5	50	45	318.42 ± 19.86	76.89 ± 3.18	0.4042 ± 0.0013	-17.16 ± 0.31	317.44	76.98	0.4022	−17.21
EUGE-NE21	6	10	3	35	32.5	239.84 ± 20.43	79.90 ± 3.57	0.3020 ± 0.0008	-12.41 ± 0.29	235.81	80.41	0.2913	−12.65
EUGE-NE22	6	20	3	35	32.5	346.21 ± 21.73	75.30 ± 2.97	0.2640 ± 0.0009	-14.87 ± 0.27	346.73	75.27	0.2647	−14.84
EUGE-NE23	6	10	10	35	32.5	275.51 ± 22.67	83.48 ± 1.99	0.2463 ± 0.0008	-15.75 ± 0.28	271.48	83.99	0.2355	−15.99
EUGE-NE24	6	20	10	35	32.5	281.88 ± 17.58	77.00 ± 1.82	0.4002 ± 0.0009	-18.69 ± 0.34	282.4	76.97	0.4009	−18.66
EUGE-NE25	2	15	6.5	20	32.5	279.68 ± 16.13	75.52 ± 2.64	0.3943 ± 0.0010	-13.30 ± 0.31	280.3	75.44	0.3960	−13.26
EUGE-NE26	10	15	6.5	20	32.5	333.82 ± 19.61	72.11 ± 2.09	0.4452 ± 0.0013	-17.30 ± 0.36	334.44	72.03	0.4469	−17.27
EUGE-NE27	2	15	6.5	50	32.5	322.81 ± 19.17	71.24 ± 1.97	0.4853 ± 0.0012	-14.55 ± 0.34	324.34	71.04	0.4895	−14.46
EUGE-NE28	10	15	6.5	50	32.5	376.95 ± 19.82	70.32 ± 2.06	0.4872 ± 0.0011	-19.03 ± 0.37	378.48	70.12	0.4914	−18.94
EUGE-NE29	6	15	3	35	20	339.18 ± 18.19	71.77 ± 2.49	0.3475 ± 0.0009	-13.01 ± 0.27	340.31	71.63	0.3504	−12.95
EUGE-NE30	6	15	10	35	20	324.85 ± 17.68	79.18 ± 2.53	0.3368 ± 0.0008	-13.50 ± 0.28	325.98	79.04	0.3397	−13.43
EUGE-NE31	6	15	3	35	45	264.1 ± 15.44	80.23 ± 3.17	0.2271 ± 0.0004	-10.02 ± 0.21	261.78	80.47	0.2220	−10.16
EUGE-NE32	6	15	10	35	45	249.77 ± 14.95	78.10 ± 2.47	0.3183 ± 0.0009	-16.70 ± 0.28	247.45	78.34	0.3132	−16.84
EUGE-NE33	2	15	6.5	35	20	313.28 ± 20.57	75.88 ± 2.73	0.4134 ± 0.0011	-12.54 ± 0.27	314.41	75.85	0.4140	−12.47
EUGE-NE34	10	15	6.5	35	20	367.42 ± 21.66	74.20 ± 2.83	0.3753 ± 0.010	-18.99 ± 0.36	368.55	74.17	0.3759	−18.92
EUGE-NE35	2	15	6.5	35	45	238.2 ± 16.83	80.06 ± 3.01	0.2795 ± 0.0008	-14.85 ± 0.24	235.88	80.41	0.2721	−14.99
EUGE-NE36	10	15	6.5	35	45	292.34 ± 19.08	77.41 ± 2.69	0.3704 ± 0.0009	-16.89 ± 0.28	290.02	77.76	0.3630	−17.03
EUGE-NE37	6	10	6.5	20	32.5	229.49 ± 17.94	83.94 ± 3.11	0.3141 ± 0.0008	-16.03 ± 0.27	222.98	84.71	0.2978	−16.42
EUGE-NE38	6	20	6.5	20	32.5	312.78 ± 21.15	75.28 ± 2.97	0.4061 ± 0.0006	-18.83 ± 0.37	314.46	75.14	0.4090	−18.73
EUGE-NE39	6	10	6.5	50	32.5	299.54 ± 18.28	77.79 ± 2.52	0.4147 ± 0.0007	-17.62 ± 0.29	297.58	78.08	0.4086	−17.74
EUGE-NE40	6	20	6.5	50	32.5	328.99 ± 22.67	75.36 ± 2.61	0.4386 ± 0.0014	-20.22 ± 0.37	327.94	75.47	0.4362	−20.28

https://doi.org/10.1021/acsomega.5c00783
ACS Omega 2025, 10, 16815−16840

Table 2. continued

Formulation code	Independent variables: Coded factors X_1	X_2	X_3	X_4	X_5	Dependent variables: Observed responses Y_1	Y_2	Y_3	Y_4	Predicted responses Y_1	Y_2	Y_3	Y_4
						Centre Points							
EUGE-NE41	6	15	6.5	35	32.5	385.83 ± 22.98	77.21 ± 2.74	0.5220 ± 0.0013	-21.14 ± 0.26	384.87	77.31	0.5200	−21.20
EUGE-NE42	6	15	6.5	35	32.5	385.83 ± 22.98	77.21 ± 2.74	0.5220 ± 0.0013	-21.14 ± 0.26	384.87	77.31	0.5200	−21.20
EUGE-NE43	6	15	6.5	35	32.5	385.83 ± 22.98	77.21 ± 2.74	0.5220 ± 0.0013	-21.14 ± 0.26	384.87	77.31	0.5200	−21.20
EUGE-NE44	6	15	6.5	35	32.5	385.83 ± 22.98	77.21 ± 2.74	0.5220 ± 0.0013	-21.14 ± 0.26	384.87	77.31	0.5200	−21.20
EUGE-NE45	6	15	6.5	35	32.5	385.83 ± 22.98	77.21 ± 2.74	0.5220 ± 0.0013	-21.14 ± 0.26	384.87	77.31	0.5200	−21.20
EUGE-NE46	6	15	6.5	35	32.5	385.83 ± 22.98	77.21 ± 2.74	0.5220 ± 0.0013	-21.14 ± 0.26	384.87	77.31	0.5200	−21.20

Table 3. Results of Regression Analysis for Responses Y_1 (Particle Size, nm), Y_2 (Transmittance, %), Y_3 (PDI), and Y_4 (Zeta Potential, mV)

quadratic model	R^2	adjusted R^2	predicted R^2	standard deviation	coefficient of variation (%)
Y_1 (eq 2)	0.9947	0.9904	0.9843	5.39	1.73
Y_2 (eq 3)	0.9909	0.9837	0.9731	0.5596	0.7287
Y_3 (eq 4)	0.9912	0.9841	0.9737	0.0118	3.07
Y_4 (eq 5)	0.9945	0.9901	0.9837	0.3218	1.95

initially reduced the globule size up to 12.5% but subsequently led to a rise in size, potentially due to the formation of smaller particles followed by agglomeration. The initial decrease in size may result from decreased interfacial tension between the two phases that helps to minimize particle agglomeration.[38] Additionally, ultrasonication plays a significant role in reducing the globule size. As the duration of ultrasonication is extended, the size of globule of the prepared nanoemulsions diminishes due to the disintegration of larger globules into smaller ones.[38]

Influence of Independent Variables on % Transmittance. For every experimental trial of EUGE-NEs, the Smix was made utilizing the ultrasonication technique, with the findings detailed in Table 2. The % transmittance varied between 70.02% and 93.60%, and the effect of the independent variables on % transmittance is demonstrated using polynomial eq 3, along with 3D and contour plots (Figure 3). As the percentage of oil increased from 2 to 10%, a corresponding decrease in transmittance (%) was observed. This decrease can be linked to the increased concentration available for encapsulating EUGE within the matrix of oil. The Smix ratio displayed a biphasic effect concerning % transmittance. At first, a rise in concentration improved % transmittance because of the enhanced solubility of PGL and decreased drug partitioning into the aqueous phase.[38] However, further increases in concentration resulted in larger globule formation and an increase in EUGE solubility within the aqueous phase, leading to a reduction in % transmittance. Increasing the ultrasonication time initially caused a decrease in globule size, followed by agglomeration, resulting in the formation of larger globules.[38] The initial increase in % transmittance is likely due to improved emulsification efficiency and a reduction in interfacial tension, which aids in the formation of smaller and more uniform globules. However, the subsequent decrease in % transmittance may result from the excessive concentration of Smix, which could lead to particle aggregation and reduced light-scattering efficiency[38] (Figure 3).

Influence of Independent Variables on PDI. The PDI of PGL-NEs was measured to range from 0.166 to 0.522. The impact of the independent variables on PDI was illustrated through polynomial eq 4, as well as 3D and contour plots (Figure 4). The oil phase demonstrated a significant effect on the PDI of the nanoemulsion. As the percentage of oil increased from 2 to 10%, the values of PDI also rose. This rise in the PDI is linked to the aggregation of particles. The second variable, Smix, also had a positive impact on the PDI. As the concentration increased from 5 to 20%, the PDI increased, which may be related to changes in globule size and subsequent agglomeration. The initial reduction in size could be attributed to a decrease in interfacial tension between the two phases, which aids in preventing particle agglomeration.[38] Additionally, ultrasonication plays a crucial role in breaking down globules. With longer ultrasonication times, the PDI of

https://doi.org/10.1021/acsomega.5c00783
ACS Omega 2025, 10, 16815−16840

Table 4. Best Optimized and Predicted Batch of EUGE-NE with Independent Variables and Dependent Variables

	Independent variables					Dependent variables			
Batch	X_1	X_2	X_3	X_4	X_5	Y_1	Y_2	Y_3	Y_4
Predicted	6.0	9.989	6.5	30	40	149.23	91.40	0.1712	−19.80
Optimized	6	10	6.5	30	40	142.4± 11.31	93.60± 5.33	0.166 ± 0.009	−19.70 ± 0.052
Some Other Characterized Parameters of EUGE-NE									
PDI		Zeta Potential (mV)		Refractive index		Viscosity (centipoise)		pH	Drug content (%)
0.166 ± 0.009		−19.70 ± 0.052		1.66 ± 0.031		39 ± 9 cP		7.20 ± 0.09	98.69 ± 0.54%

Table 5. Fit Summary for Responses Y_1, Y_2, Y_3, and Y_4 and Regression Equations

Models	Sequential p-value	Adjusted R^2	Predicted R^2	Remarks
Response 1: Y_1 (Globule Size)				
Linear	0.0021	0.2859	0.2131	
2FI	0.0453	0.4521	0.4050	
Quadratic	<0.0001	0.9904	0.9843	Suggested
Cubic	<0.0001	1.0000		Aliased
Response 2: Y_2 (%Transmittance)				
Linear	0.0117	0.2111	0.0517	
2FI	0.2651	0.2694	−0.3203	
Quadratic	<0.0001	0.9837	0.9731	Suggested
Cubic	<0.0001	0.9997		Aliased
Response 3: Y_3 (Polydispersity Index)				
Linear	0.2639	0.0373	−0.0759	
2FI	0.1971	0.1396	−0.0806	
Quadratic	<0.0001	0.9841	0.9737	Suggested
Cubic	<0.0001	0.9997		Aliased
Response 4: Y_4 (Zeta Potential)				
Linear	0.0062	0.2399	0.1642	
2FI	0.9980	0.0370	−0.2803	
Quadratic	<0.0001	0.9901	0.9837	Suggested
Cubic	<0.0001	1.0000		Aliased

the prepared nanoemulsion overall, the PDI generally decreased as globules fragmented into smaller sizes; however, some cases of increased PDI were also noted.[38] Additionally, ultrasonication plays a crucial role in breaking down the globules. With longer ultrasonication times, the PDI of the prepared nanoemulsion overall, the PDI generally decreased as globules fragmented into smaller sizes; however, some cases of increased PDI were also noted.[38]

Influence of Independent Variables on ZP (mV). The ZP for all the formulated nanoemulsions was measured to be in the range of −9.51 ± 0.26 to −21.14 ± 0.26 mV. It was observed that the quantity of oil had a significant impact on the zeta potential, whereas sonication time and the Smix ratio exhibited a minimal effect. The results of the quadratic model, represented by eq 5, were examined utilizing ANOVA, yielding a high R^2 value of 0.9945 (Table 3). The zeta potential demonstrated a negative effect associated with the combined influence of oil percentage, sonication time, and Smix, as indicated by the negative interactions [$-X_1X_2$, $-X_1X_3$, $-X_1X_4$, $-X_2X_3$, $-X_2X_4$, $-X_3X_4$, $-X_3X_5$, $-X_4X_5$]. Conversely, the zeta potential showed negative values correlating with the positive effects of oil percentage and temperature ($+X_1X_5$) as well as Smix (% v/v) in conjunction with the temperature ($+X_2X_5$). All the prepared nanoemulsions exhibited a clear and transparent appearance, with % transmittance values ranging from 70.02 ± 2.72% to 93.60 ± 5.33%,[38] confirming successful nanoemulsion formation. The high transmittance suggests smaller droplet sizes, contributing to the improved solubility, stability, and permeability. The development of EUGE-NE involved Clove Oil, a mixture of Tween-80 as a surfactant, and PEG 400 as a cosurfactant, which played a crucial role in reducing interfacial tension and preventing droplet aggregation. The ultrasonication process further optimized the droplet size, enhancing transparency and stability. Since intranasal drug delivery relies on efficient mucosal absorption, higher transmittance indicates better permeability and bioavailability. The formulations with the highest clarity are expected to provide superior drug uptake into the systemic circulation and brain tissue. Overall, the results confirm the successful development of stable nanoemulsions with optimal properties for intranasal drug delivery.[38] For the interaction between oil and Smix ($-X_1X_2$), an increase in the oil concentration enhances the hydrophobic content, which modifies the surface charge distribution on the globules. At the same time, higher Smix levels improve emulsification efficiency but may neutralize charges at the interface, leading to a reduction in the overall ZP. For the interaction between oil and ultrasonication time ($-X_1X_3$), extended sonication decreases the globule size, whereas higher oil concentrations encourage aggregation. This combination disrupts the equilibrium of charged species, reducing electrostatic repulsion and thereby lowering the ZP. For the interaction between ultrasonication time and intensity ($-X_3X_4$): When both ultrasonication time and intensity are high, the excessive energy input can result in globule agglomeration due to increased collision frequency, diminishing the ZP. The predominantly negative ZP values indicate that the nanoemulsions achieve stabilization through electrostatic mechanisms. However, factors such as oil concentration, Smix ratio, and sonication parameters significantly influence the surface charge distribution and the electrostatic stability of the globules (Figure 5).

3D-Response Surface and Contour Plot. A total of 46 experimental trials were carried out using BBD optimization software, incorporating five factors at four levels, with the findings displayed in Tables 2, 3, 4, and 5. The impact of independent variables on a single response at a time was illustrated through 3D and contour plots generated by the BBD software (Figures 2−5). Several statistical parameters, such as regression (R^2), adjusted R^2, predicted R^2, standard deviation (SD), and % coefficient of variation (CV), were computed for the regression, lack of fit, and residuals of the optimal quadratic model, as illustrated in Tables 3− 5. The statistical summaries for the quadratic model related to both responses are presented in Tables 3 and 5. Significant differences in R^2, adjusted R^2, and predicted R^2 values were noted for all models of each response, with the quadratic model exhibiting the highest R^2 value, confirming it as the best-fit model for each response.

Findings from the response fitting indicate the optimized EUGE-NE, characterized by maximum average globule size

https://doi.org/10.1021/acsomega.5c00783
ACS Omega 2025, 10, 16815−16840

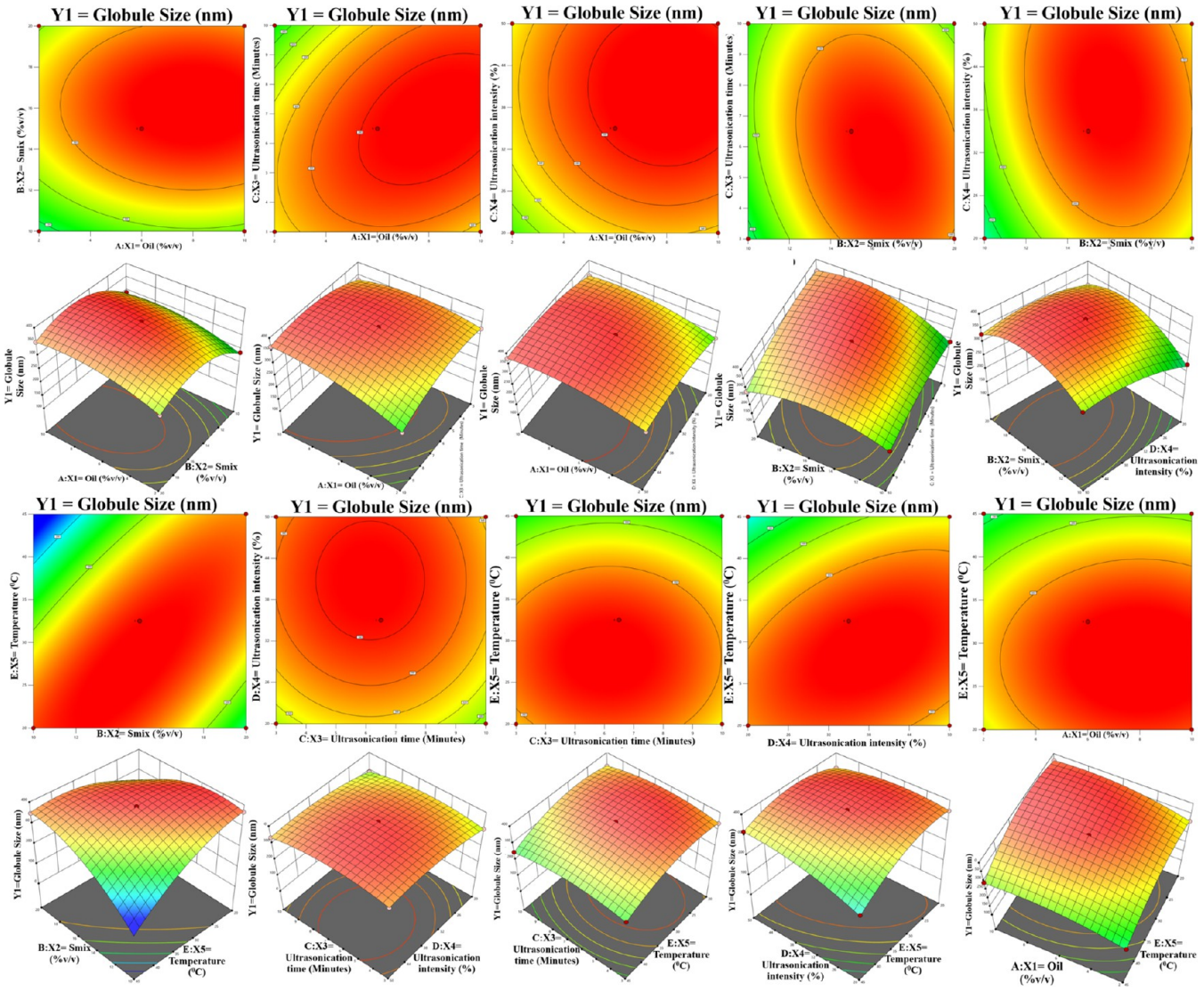

Figure 2. Effect of clove oil: oil phase (A), Smix (B) [Tween 80: surfactant, PEG 400: cosurfactant], and ultrasonication speed (C) on globule size (Y_1).

(nm), % transmittance, PDI, and zeta potential in mV. The optimized nanoemulsion was obtained through point prediction using BBD software, which included Clove-Oil (6.0%), a Smix ratio of Tween-80 (surfactant) and PEG 400 (cosurfactant) at 3:1 (10%), an ultrasonication duration of 6.5 min, an ultrasonication intensity of 30%, and a temperature of 40 °C. The actual and predicted values for globule size (nm), % transmittance, PDI, and zeta potential (mV) of EUGE-NE were recorded as 142.4 ± 11.31 nm, 93.60 ± 5.33%, 0.1660 ± 0.0009, and −19.70 ± 0.052 mV, respectively (Table 2). The strong correlation between the predicted and actual values indicates the effectiveness of the optimization method used for preparing EUGE-NE. Overall, the globule size, %transmittance, PDI, and ZP of EUGE-NE were determined to be 142.4 nm, 93.60%, 0.166, and − 19.70 mV, respectively (Table 2).

Factors can influence the levels of retraction in ways not predicted by the regression equation. This discrepancy may arise from changes made at different points during formulation or from simultaneous modifications of multiple parameters. The interaction effects of X_1, X_2, X_3, X_4, and X_5 were beneficial for all four outcomes assessed. Each of the dependent variables (Y_1, Y_2, Y_3, and Y_4) exhibited values greater than 0.9909 (Table 3) in their respective regression equations, indicating a strong correlation. Additionally, the projected and adjusted Y_2 values for each response showed a very close alignment (Figure 6). These results support the statistical validity and practical relevance of these equations for optimizing nanoemulsions.

The results obtained through response surface methodology (RSM) were further assessed for a model fit. Four checkpoint formulations were selected (Table 6) and analyzed for globule size (GS), % transmittance, PDI, and ZP. The validity of the RSM was determined by calculating the percentage prediction error, which involved comparing the experimental values with the predicted values produced via the software. When the experimental values for all responses were compared to the predicted values, the percentage prediction error ranged from −3.34% to +2.10%. The small prediction error indicates a strong fit between the experimental and theoretical values, confirming the high predictive capability of the RSM design for optimizing nanoemulsions.

https://doi.org/10.1021/acsomega.5c00783
ACS Omega 2025, 10, 16815−16840

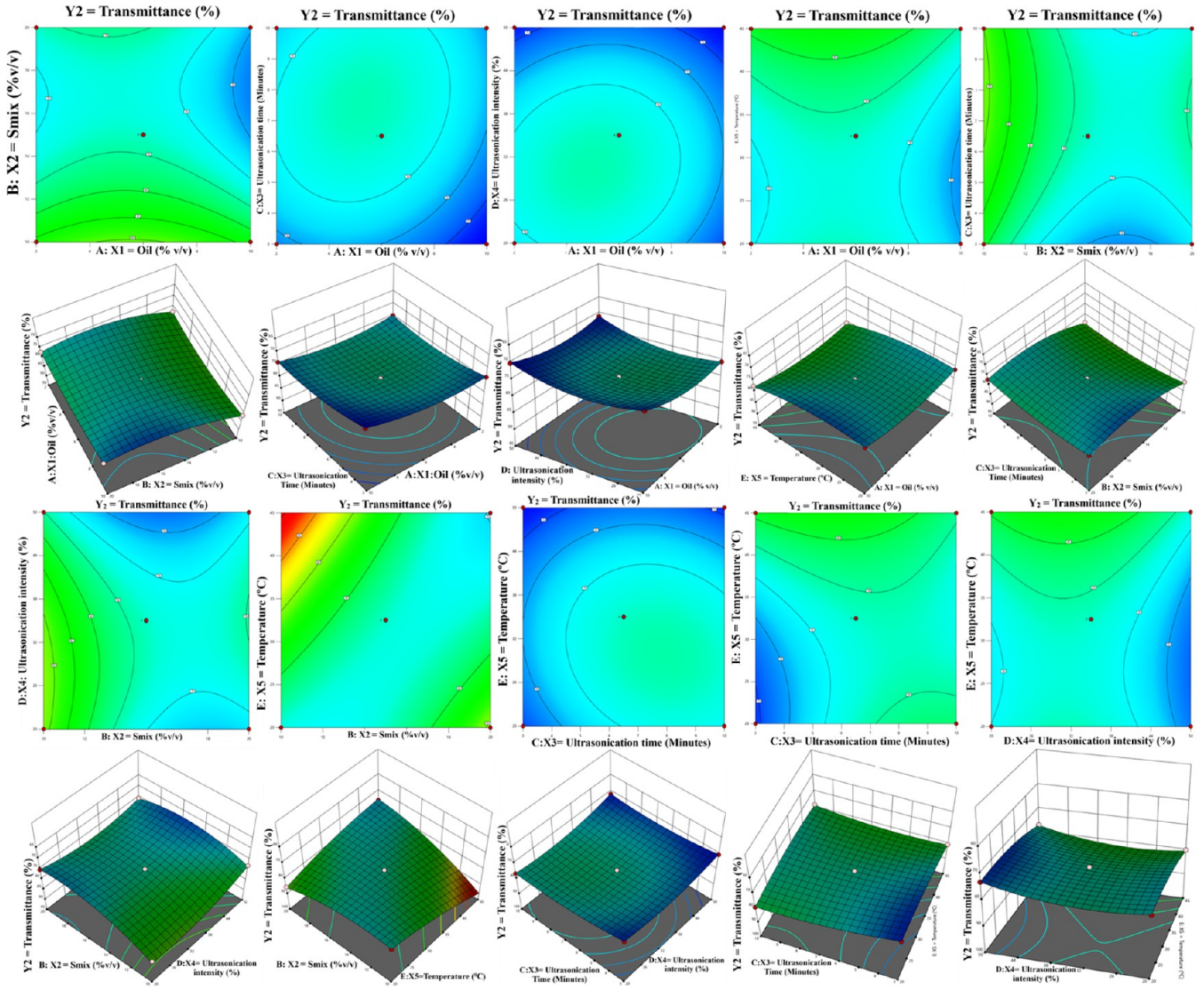

Figure 3. Effect of Capryol 90: oil phase (A), Smix (B) [Tween 80: surfactant, PEG 400: cosurfactant], and ultrasonication speed (C) on percentage transmittance (Y_2).

The optimized values for the three formulation factors were determined using Design Expert Software (BBD), which applied constraints to achieve a target globule size of ≤ 200 nm (ideal for intranasal drug delivery targeting the brain) and a ZP of ≤ + 25 mV to confirm stability while maximizing entrapment efficiency.

Figures 7−8910 illustrate the graphical representations of each optimal solution. The four dependent variables of the nanoemulsions were optimized based on the predicted values derived from constraints and quadratic equations using Box−Behnken Design software. The final composition for the checkpoint formulations, which includes globule size, % transmittance, PDI, and ZP, is as follows: 6% clove oil, 10% Smix, 6.5 min of ultrasonication, 30% intensity of ultrasonication, and a 40 °C temperature (Tables 4−6). The Box−Behnken Design software recommended the optimized formulation of clove oil, which consists of 6.0% clove oil, 10% Smix, a 6.5 min ultrasonication time, 30% ultrasonication intensity, and a temperature of 40 °C, all determined based on the constraints and quadratic equations related to the four dependent variables (Table 3). Furthermore, the optimized values for globule size (142.4 nm), % transmittance (93.60%), PDI (0.166), and ZP (−19.70 mV) were associated with a wishing of 0.9996. These values were derived from the experimental results of the nanoemulsions to validate their globule size, % transmittance, PDI, and ZP, as shown in Tables 4−6 and Figures 7−V−10.

Enhancing the bioavailability of the brain is crucial for treating depression and sleep disorders. The uptake of cells was improved by coating a novel natural biodegradable chitosan (CHS) onto an Eugenol nanoemulsion (EUGE-NE 11) at various concentrations. We employed the method explained by Ahmad et al. to coat the Eugenol nanoemulsion with chitosan, aiming for targeted delivery of Eugenol to the brain via intranasal administration. After coating, the zeta potential of the chitosan-coated Eugenol nanoemulsion (referred to as CHS-EUGE-NE) shifted from negative to positive, with only a minor change in globule size (remaining below 200 nm) and a PDI of 0.263 (Figures 11 and 12). The sonication process contributed to a decrease in globule size to the nanometer range while maintaining a low PDI. The optimized Eugenol-NE indicated a globule size of 142.4 ± 11.31 nm, with the

https://doi.org/10.1021/acsomega.5c00783
ACS Omega 2025, 10, 16815−16840

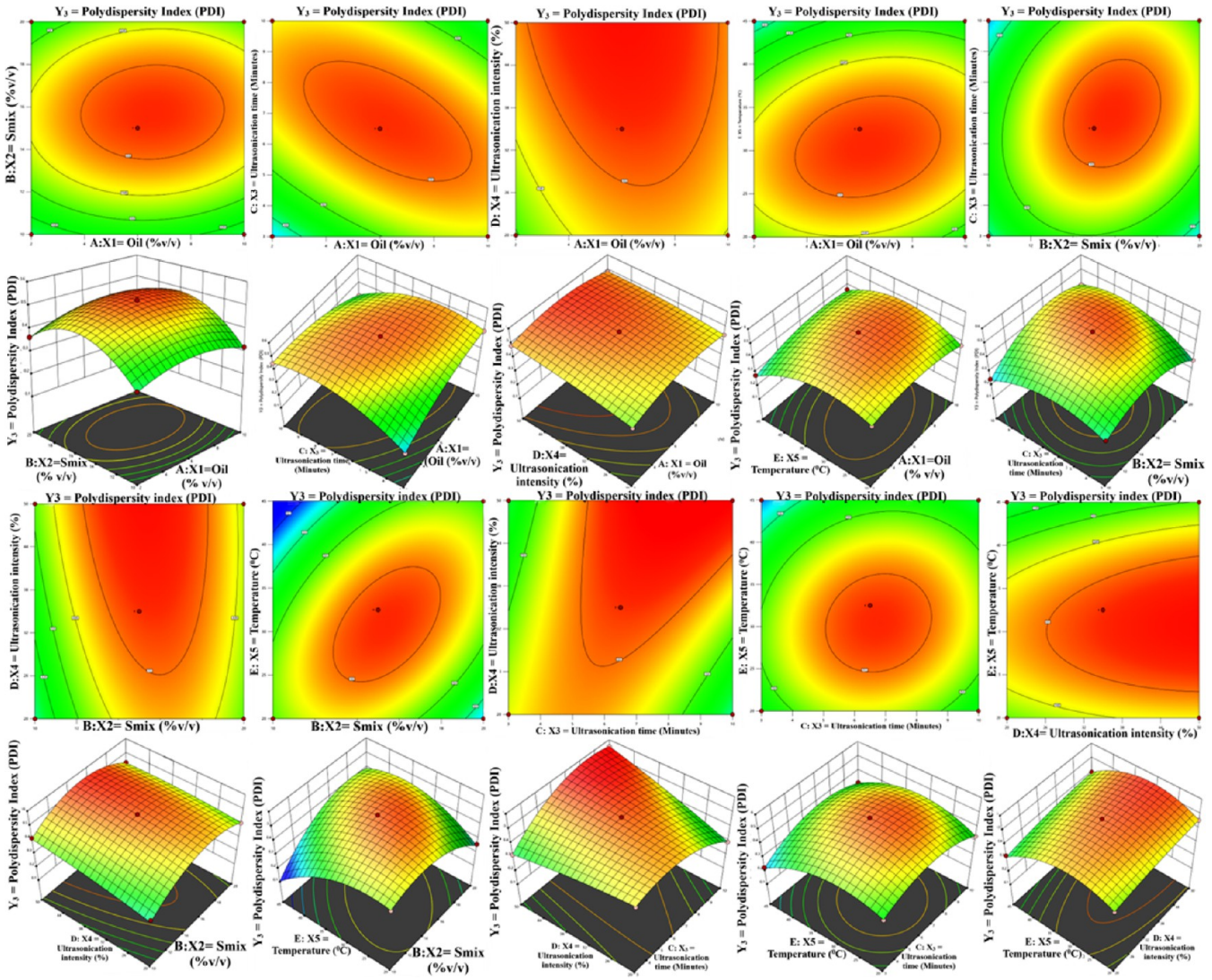

Figure 4. Effect of Capryol 90: oil phase (A), Smix (B) [Tween 80: surfactant, PEG 400: cosurfactant], and ultrasonication speed (C) on the polydispersity index (PDI) (Y_3).

loading of Eugenol not affecting the size significantly. Initially, the globule size of EUGE-NE was recorded at 142.4 ± 11.31 nm, and upon the addition of CHS, it increased to 198.6 ± 13.74 nm (Figure 11).[38] This slight increase in globule size due to the chitosan coating has been previously documented, indicating that the addition of CHS as a polymer to EUGE-NE contributes to the enhancement of globule size.[38] We observed a polydispersity index (PDI) value of less than 0.263 ± 0.0007, indicating a narrow distribution of globule sizes within the suspension. Additionally, the zeta potential (ZP) ranged from −19.70 ± 0.052 to +23.10 ± 1.13, reflecting a transition from negative to positive values (Figure 12). The zeta potential became positive after coating the Eugenol nanoemulsion (EUGE-NE) with the chitosan (CHS), likely due to the presence of amine groups in the chitosan structure.[28,42] The polydispersity index (PDI) for CHS-EUGE-NE was found to be less than 0.263, indicating the monodisperse nature of the nanoemulsion. The zeta potential (ZP) of the Eugenol nanoemulsion (EUGE-NE) consistently exhibited a negative charge of −19.70 ± 0.052 mV (Figure 12). After the application of chitosan (CHS) coating on EUGE-NE, the surface charge changed significantly to a positive value of +23.10 ± 1.13.[28,38,42] Although the globule size increased slightly following the CHS coating, there was minimal change in the PDI. This suggests that CHS-EUGE-NE is unlikely to experience agglomeration during the preparation of the nanoemulsion.

Nanoemulsion Characterization. *ZP, Globule Size, Polydispersity Index, and % Transmittance.* Permeation of the nanoemulsion is enhanced by the smaller globule size, which increases the overall surface area of the globules. Opt-EUGE-NE demonstrated a globule size of 142.4 ± 11.31 nm (Tables 2, 4 and Figure 11A).[52] The polydispersity index (PDI) was measured at 0.166 ± 0.009, indicating a narrow distribution of globule sizes.[52] The zeta potential (ZP) for Opt-EUGE-NE was found to be −19.70 ± 0.052 mV (Figure 12A, Tables 2 and 4). This small negative charge can be accredited to the presence of nonionic surfactants and steric hindrance effects. The stability of the nanoemulsion and its globule size are crucial factors influencing the percentage of transmittance. Any variations in these parameters can affect the size distribution. Opt-EUGE-NE exhibited a transmittance of 93.60 ± 5.33%, as presented in Tables 2 and 4, indicating a clear and uniform distribution of the oil phase.[64]

https://doi.org/10.1021/acsomega.5c00783
ACS Omega 2025, 10, 16815−16840

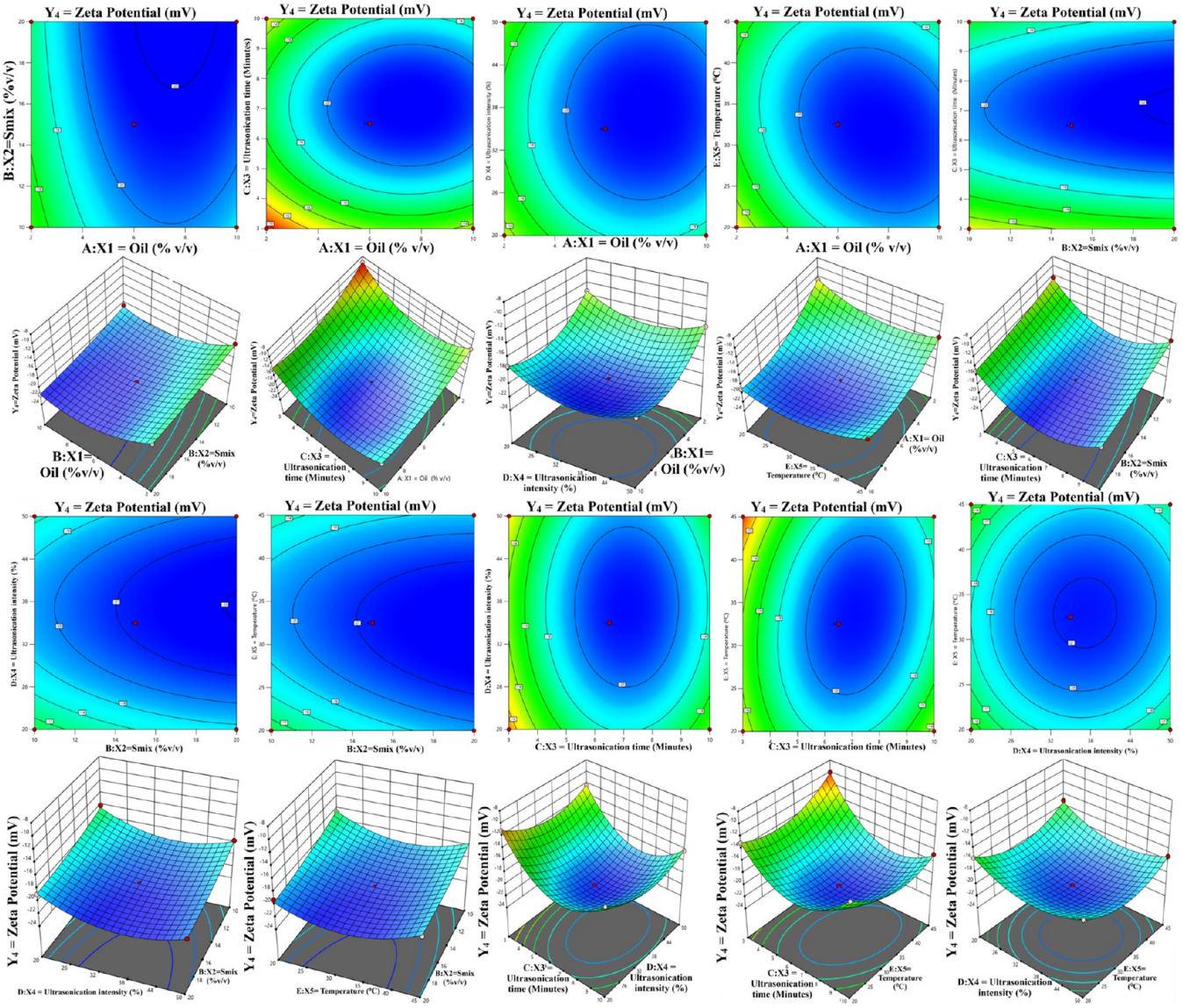

Figure 5. Effect of Capryol 90: oil phase (A), Smix (B) [Tween 80: surfactant, PEG 400: cosurfactant], and ultrasonication speed (C) on zeta potential (mV) (Y_4).

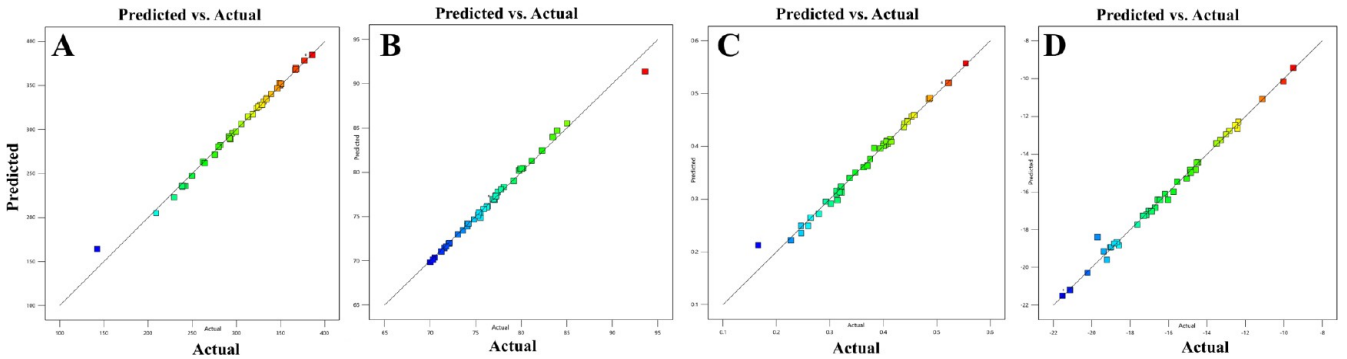

Figure 6. Linear corelation plot between the actual and predicted values of (A) mean globule size (Y_1), (B) transmittance (Y_2), (C) polydispersity index (PDI) (Y_3), and (D) zeta potential (mV) (Y_4).

Impact of Mucoadhesive Natural Biodegradable Chitosan on Optimized Nanoemulsion. A concentration of chitosan (1%w/v) was utilized to formulate a mucoadhesive known as CHS-EUGE-NE. The optimized mucoadhesive formulation demonstrated promising results, including a globule size of 198.6 ± 13.74 nm, a positive zeta potential of +23.10 ± 1.13 mV, and a PDI of 0.263 ± 0.0007 (Figures 11B and 12B). TEM confirmed that the globules were below 200 nm in size and exhibited a spherical shape, consistent with measurements obtained from the zeta sizer (Figures 11

https://doi.org/10.1021/acsomega.5c00783
ACS Omega 2025, 10, 16815−16840

Table 6. Different Checkpoint Formulations, Predicted and Experimental Values of Response Variables and % Prediction Error for Nanoemulsions

#	Checkpoint formulations (*X1*:*X2*:*X3*:*X4*:*X5*)	Response variable	Experimental values	Predicted values	% Prediction Error
1	6.5:10.5:7.0:32.0:45	Y_1 = GS: nm	161.63	155.64	+2.10
		Y_2 = Transmittance: %	88.06	86.37	−1.61
		Y_3 = PDI	0.178	0.175	+1.76
		Y_4 = ZP: mV	−21.30	−23.41	−1.03
2	6.0:10:6.5:30:40	Y_1 = GS: nm	142.4	149.23	−2.79
		Y_2 = Transmittance: %	93.60	91.40	+1.48
		Y_3 = PDI	0.166	0.171	−0.67
		Y_4 = ZP: mV	−19.70	−19.80	+0.13
3	5.5:9.5:6.0:28:37	Y_1 = GS: nm	158.67	149.23	−2.79
		Y_2 = Transmittance: %	81.05	80.31	+0.39
		Y_3 = PDI	0.220	0.219	+0.59
		Y_4 = ZP: mV	−23.16	−24.61	+1.09
4	5.0:9.0:5.5:24:34	Y_1 = GS: nm	219.64	226.17	−3.34
		Y_2 = Transmittance: %	76.97	79.01	−2.87
		Y_3 = PDI	0.250	0.255	+1.02
		Y_4 = ZP: mV	−24.65	−23.11	−1.01

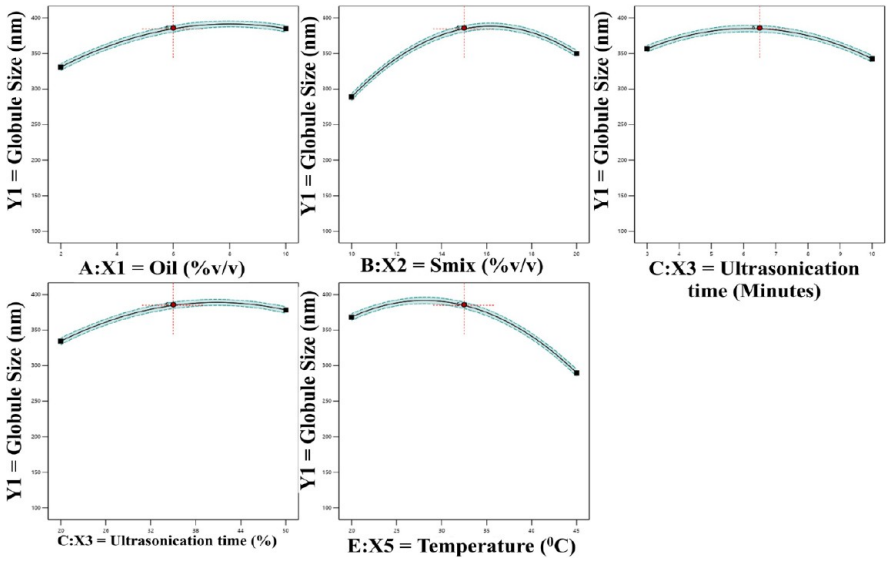

Figure 7. Graphical view of overall desirability score and each optimal solution for globule size.

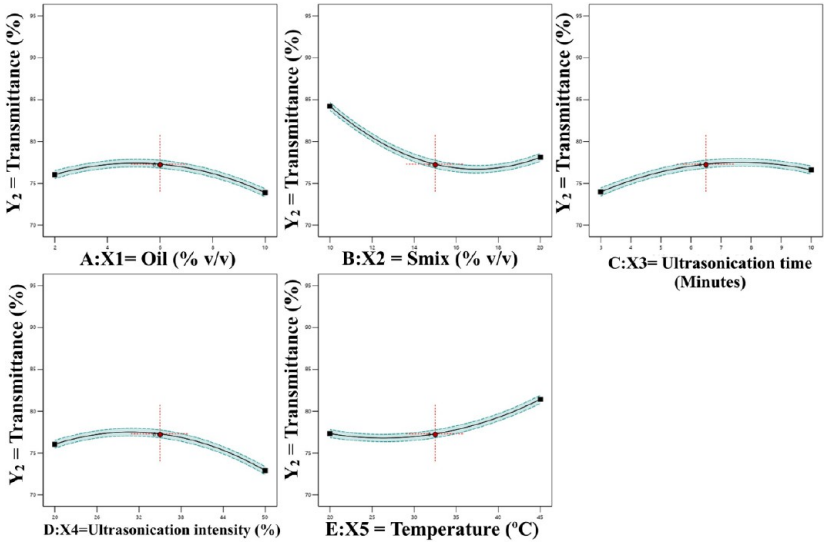

Figure 8. Graphical view of overall desirability score and each optimal solution for % transmittance.

https://doi.org/10.1021/acsomega.5c00783
ACS Omega 2025, 10, 16815−16840

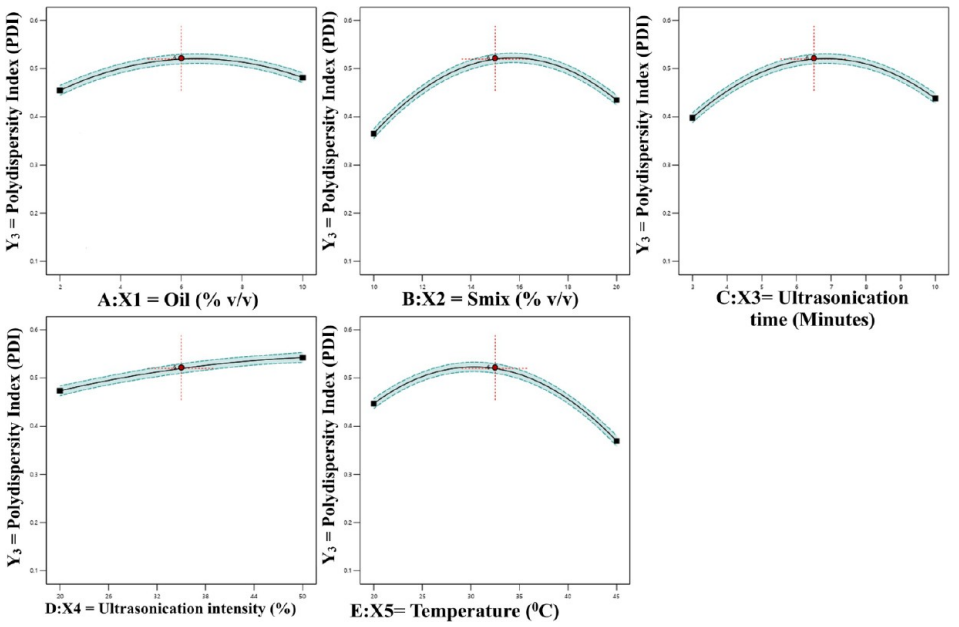

Figure 9. Graphical view of overall desirability score and each optimal solution for PDI.

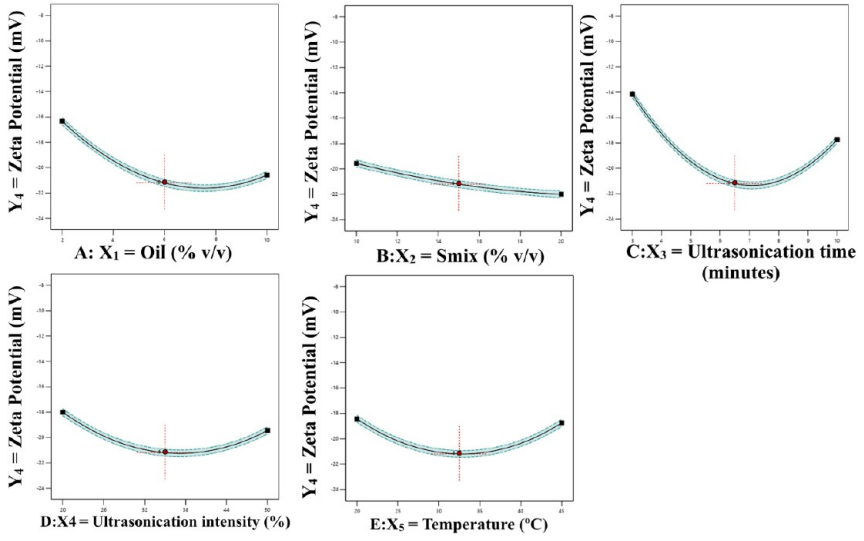

Figure 10. Graphical view of overall desirability score and each optimal solution for zeta potential.

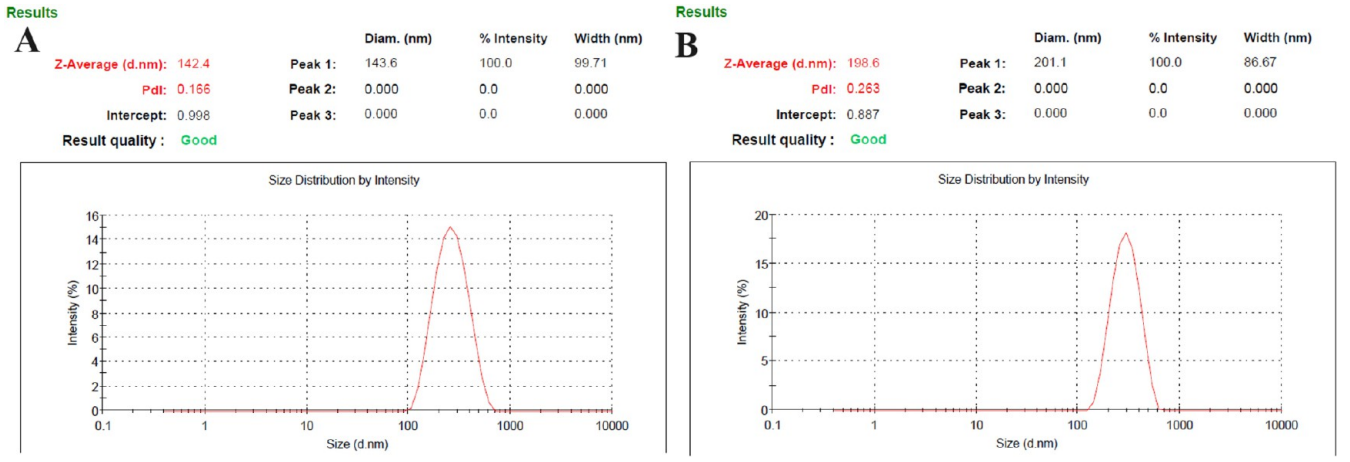

Figure 11. Dynamic light scattering techniques for determining the particle size distributions of EUGE-NE (A) and CHS- EUGE-NE (B).

https://doi.org/10.1021/acsomega.5c00783
ACS Omega 2025, 10, 16815−16840

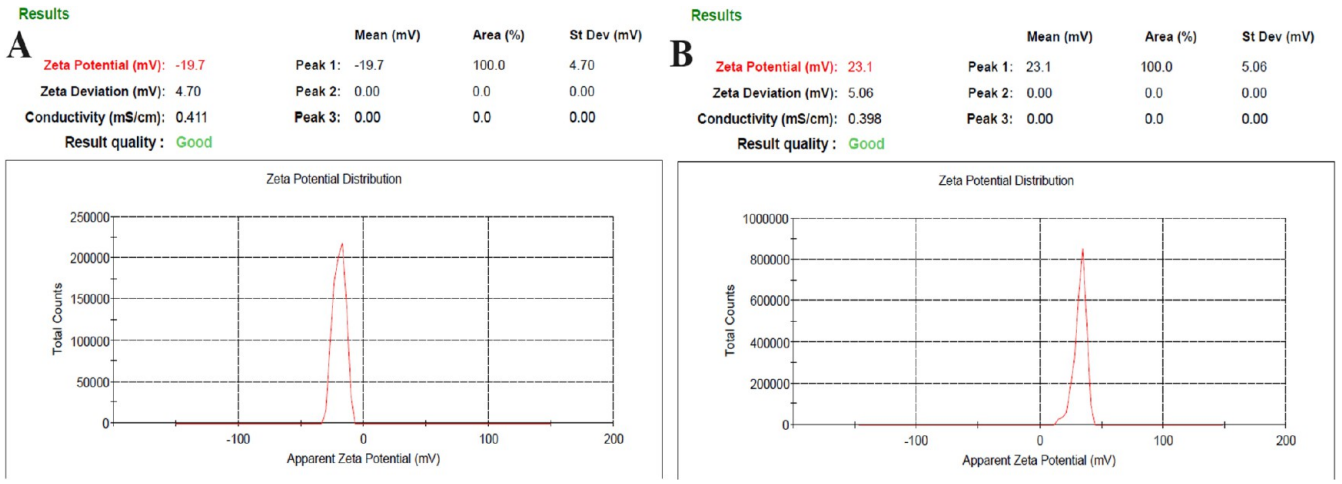

Figure 12. Dynamic light scattering techniques for determining the zeta potential of EUGE-NE (A) and CHS- EUGE-NE (B).

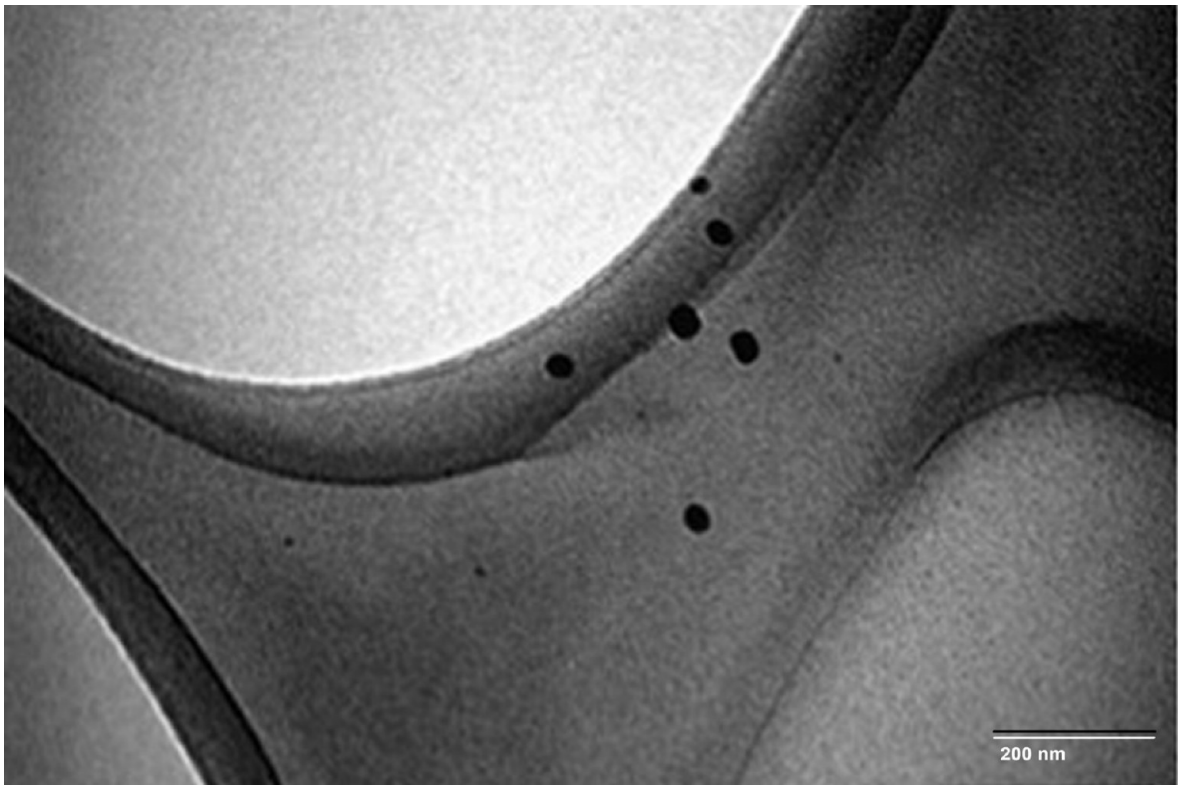

Figure 13. Transmission electron microscopy (TEM) image of CHS-EUG-NE.

and12). Additionally, the CHS-EUGE mucoadhesive nanoemulsion displayed a low PDI value, indicating a narrow size globules distribution. Tests for stability, conducted thermodynamically, yielded satisfactory results for the PDI of CHS-EUGE mucoadhesive nanoemulsion, maintaining a size of less than 200 nm (Figure 11B). The viscosity of EUGE-NE11 was measured at 39 ± 9 cP, while the CHS-EUGE mucoadhesive nanoemulsion had a slightly higher viscosity of 42.7 ± 7.1 cP. These results indicate that chitosan improves the mucoadhesive properties of the optimized EUGE-NE11 formulation, which is a primary objective of our research. The positive charge of chitosan interacts with the negatively charged mucus, resulting in prolonged retention time at the treatment site.[65]

TEM Analysis. The optimized mucoadhesive CHS-EUGE-NE displayed a round and smooth surface, as revealed by transmission electron microscopy (TEM) (Figure 13). The globules were observed to be spherical in shape, with size < 200 nm, specifically measuring 198.6 ± 13.74 nm (Figure 11B). No aggregation was noted in opt-CHS-EUGE-NE, which maintained a distinct spherical globular structure (Figure 11B).

Other Characterization Parameters. The optimized EUGE-nanoemulsion globule size was further validated using a zetasizer. The opt-CHS-MLT-NE demonstrated a pH of 7.20 ± 0.09, which falls within the ideal range of 5.0 to 7.50 for compatibility with human mucosa, indicating that it is nonirritating based on parameters such as conductivity,

https://doi.org/10.1021/acsomega.5c00783
ACS Omega 2025, 10, 16815−16840

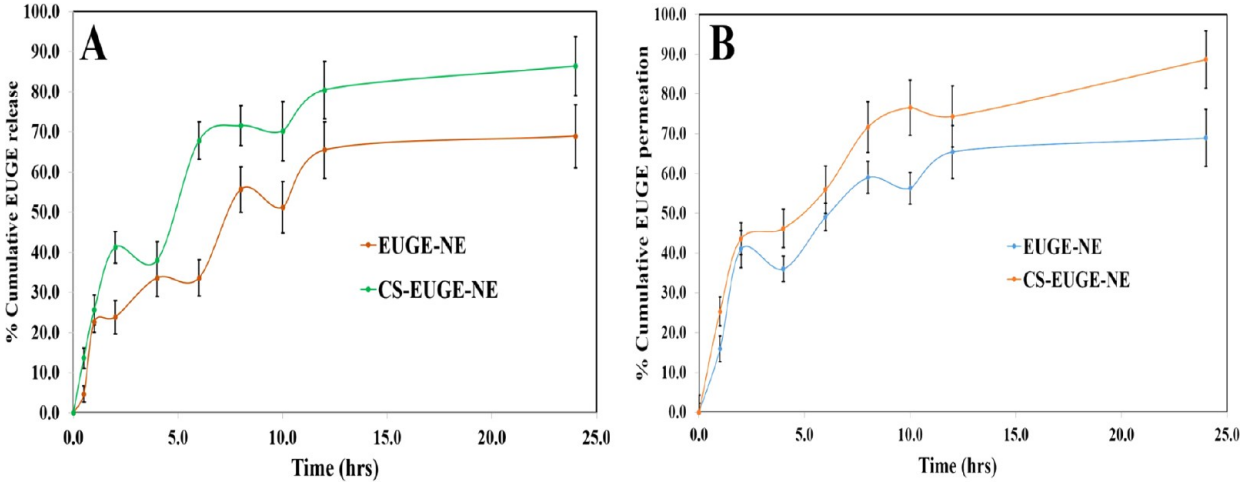

Figure 14. Cumulative percentage release of Eugenol from CHS-EUGE-NE as compared to EUGE-NE: (A). Ex vivo permeation profiles of developed CHS- EUGE-NE as compared to EUGE-NE through goat nasal mucosa (B).

Table 7. EUGE-NE Showed Stability Results After Their Optimizations

	Optimized EUGE -NE (sonication present) (EUGE − NE11)		Optimized EUGE-NEW11 (No sonication) (EUGE-NEW11)	
Duration (weeks)	Globule size (nm) (n = 3)	PDI (n = 3)	Globule size (nm) (n = 3)	PDI (n = 3)
0	142.40 ± 6.31	0.166 ± 0.0006	261.24 ± 11.24	0.242 ± 0.041
2	146.49 ± 5.78	0.169 ± 0.0004	282.69 ± 12.41	0.367 ± 0.078
4	150.37 ± 6.01	0.172 ± 0.0007	301.09 ± 12.08	0.563 ± 0.079
6	154.89 ± 5.37	0.174 ± 0.0009	393.11 ± 22.09	0.793 ± 0.091
8	161.83 ± 6.49	0.179 ± 0.0010	468.18 ± 25.19	0.991 ± 0.098
12	169.47 ± 4.71	0.181 ± 0.0009	Phase Separation	
14	176.10 ± 5.38	0.185 ± 0.0013	Phase Separation	

refractive index, viscosity, pH.[38] The isotropic nature of the nanoemulsion and the chemical interactions among the excipients were confirmed through value of RI, with the opt-CHS-EUGE-NE showing an RI of 1.706 ± 0.039, indicating a clear isotropic characteristic of the formulation.[38] Additionally, a classic dye test was conducted using opt-CHS-EUGE-NE, although the results are not presented here. Methylene blue, a water-soluble dye, penetrated the formulation within a set time frame, while methyl red exhibited a comparatively lower diffusion rate. The findings support that the opt-CHS-MLT-NE is an o/w nanoemulsion.[38]

An In Vitro Release Study. The release of EUGE from opt-EUGE-NE and opt-CHS-EUGE-NE is illustrated in Figure 14A. The opt-CHS-EUGE-NE demonstrated a significantly controlled release of Eugenol, achieving a maximum of 86.43 ± 7.36%, compared to a lower release of 68.94 ± 7.89% from opt-EUGE-NE at the 24-h mark. The enhanced release observed with opt-CHS-EUGE-NE can be accredited to the nanosized globules encapsulated via CHS, which increases the surface area available for release.[26,33] This release profile is crucial for achieving a rapid initial effect, providing a loading dose followed by a sustained release of Eugenol at the targeted site. The Korsmeyer-Peppas model was employed to analyze the release kinetics of opt-CHS-EUGE-NE, yielding a coefficient of determination (r^2) of 0.9906. The release exponent (n = 0.181) indicates a Fickian diffusion mechanism governing the release pattern of Eugenol from the formulation.[52]

Ex Vivo Permeation Study. The permeation study was conducted on nasal mucosa using opt-EUGE-NE and opt-CHS-EUGE-NE, as shown in Figure 14B. The Eugenol permeated through freshly collected goat nasal mucosa from a local slaughterhouse, with opt-EUGE-NE demonstrating a permeation rate of 68.94 ± 7.21%, while opt-CHS-EUGE-NE exhibited a higher rate of 88.64 ± 7.25% after 24 h. The controlled release of Eugenol in vitro, along with the enhanced permeation (ex vivo) via nasal tissues, is credited to the capping of Eugenol within lipid globules of the nanoemulsion, facilitating both transcellular and paracellular pathways.[38] Opt-CHS-EUGE-NE showed a greater steady-state flux of 7.06 ± 0.19 μg cm^{-2} h^{-1} compared to opt-EUGE-NE, which had a flux of 4.39 ± 0.47 μg cm^{-2} h^{-1}. Additionally, the permeability coefficient for opt-CHS-EUGE-NE was 6.92 × 10^{-3} ± 1.99 μg cm^{-2} h^{-1}, significantly higher than that of opt-EUGE-NE, which was 3.98 × 10^{-3} ± 1.67 μg cm^{-2} h^{-1}. The enhancement ratio of 2.36 for opt-CHS-EUGE-NE indicates an excellent permeation improvement due to the chitosan coating (Figure 14B). The mucoadhesive properties of the chitosan-coated Eugenol nanoemulsion contributed to an extended retention time in the nasal mucosa, facilitating prolonged drug action at the target site.[38,65] Finally, CHS-EUGE-NE (p < 0.01) showed more significant results compared to EUGE-NE.

Storage Stability Conditions for Optimized Nanoemulsion. The optimized nanoemulsion, Opt-EUGE-NE11, was produced using ultrasonication and demonstrated stability for up to 14 weeks. In contrast, the formulation created without ultrasonication showed stability for only 8 weeks. The globule size of Opt-EUGE-NE11 measured at 142.40 ± 6.31 nm, and its polydispersity index (PDI) of 0.166 ± 0.0006 increased notably during the first 4 weeks, as presented in Table 7. This increase can be attributed to turbulence generated during ultrasonication, which accelerated the rate of Ostwald ripening.

https://doi.org/10.1021/acsomega.5c00783
ACS Omega 2025, 10, 16815−16840

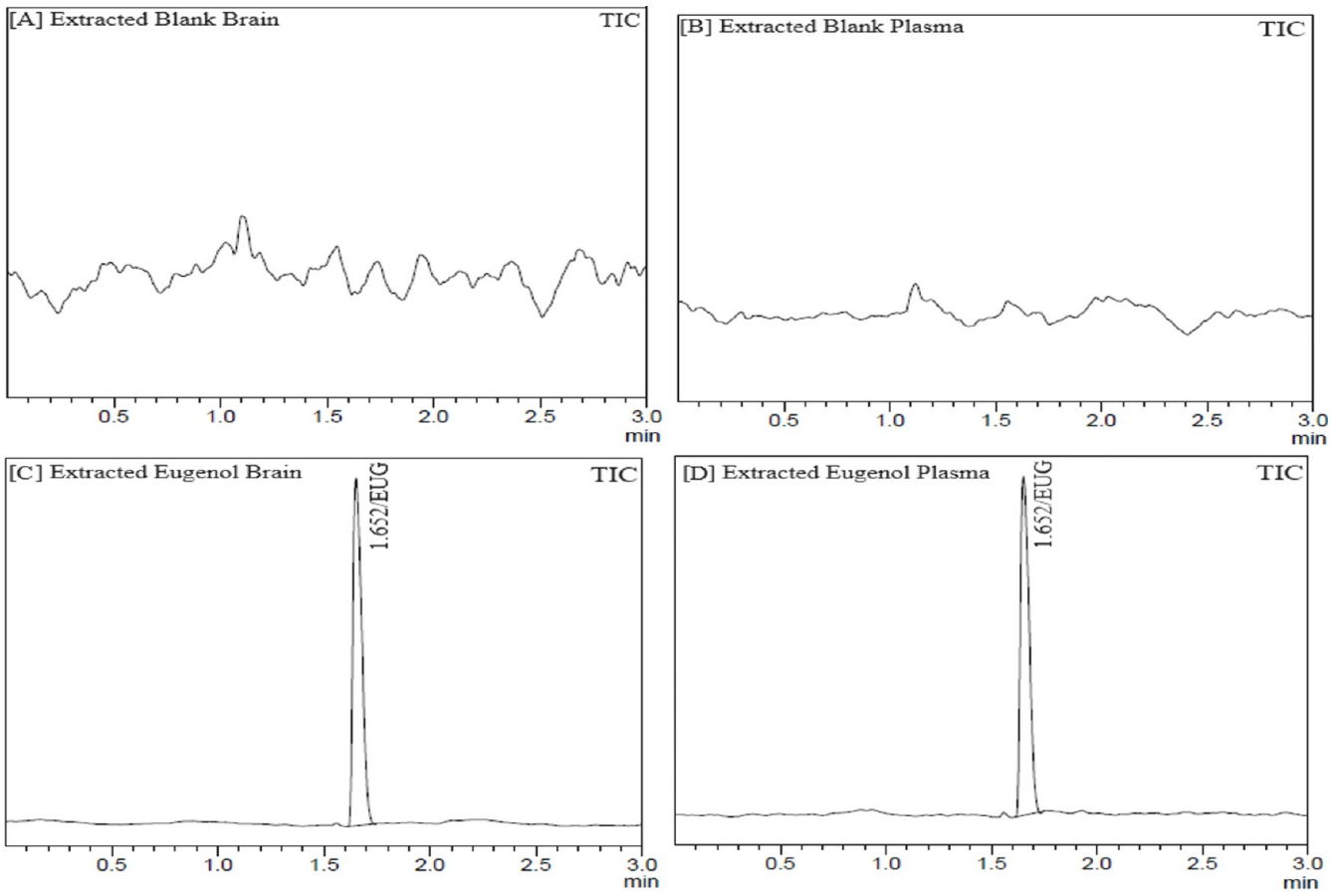

Figure 15. Typical chromatograms of extracted blank plasma (A), extracted blank brain homogenate (B), extracted eugenol brain (EUG) (C), and extracted eugenol plasma (D).

Table 8. Validation: Precision and Accuracy Data for Eugenol (EUGE) in the Plasma and Brain Homogenates[a]

			Intrabatch precision			Interbatch precision			
Biomatrix	Quality Controls Samples	Theoretical Concentration (ng mL^{-1}) or (ng g^{-1})	Observed Concentration (ng mL^{-1}) or (ng g^{-1}) ± SD.	Accuracy[b] (%)	Precision[c] (%C.V.)	Observed Concentration (ng mL^{-1}) or (ng g^{-1}) ± SD.	Accuracy[b] (%)	Precision[c] (%C.V.)	Recovery[d] (%)
Brain Homogenate	LOQQC	1.01	1.00 ± 0.011	99.01	1.10	1.00 ± 0.016	90.91	1.60	79.52
	LQC	2.92	2.91 ± 0.051	99.66	1.75	2.90 ± 0.055	99.32	1.90	80.39
	MQC	1250.0	1245.27 ± 19.33	99.62	1.55	1243.64 ± 21.37	99.42	1.72	79.99
	HQC	2400.0	2395.97 ± 43.98	99.83	1.84	2391.41 ± 44.28	99.64	1.85	82.36
Plasma	LOQQC	1.01	0.99 ± 0.013	98.02	1.31	0.98 ± 0.017	97.03	1.73	79.01
	LQC	2.92	2.90 ± 0.054	99.32	1.86	2.91 ± 0.061	99.66	2.10	81.22
	MQC	1250.0	1246.29 ± 22.63	99.70	1.82	1233.62 ± 25.94	98.69	2.10	84.06
	HQC	2400.0	2392.36 ± 39.65	99.68	1.66	2381.64 ± 41.83	99.24	1.76	84.69

[a](Mean ± SD) are derived from 6 replicates. [b]Accuracy (%) = Mean value of [(mean observed concentration)/(theoretical concentration)] × 100. [c]Precision (%): Coefficient of variance (percentage) = standard deviation divided by mean concentration found × 100. [d]Recovery (%) = Mean value of (peak height (mV) obtained from extracted biological sample)/(peak height (mV) obtained from aqueous sample) × 100.

During this process, the globule size increases, while the PDI indicates a growing uneven distribution of globule sizes.

Between 6 and 8 weeks, we observed an increase in globule size, but the PDI showed only slight changes, confirming the stability of nanoemulsions. However, after 12 weeks, there was a significant increase in globule size. For the formulation without ultrasonication (EUGE-NEW11), the initial measurements showed a globule size of 261.24 ± 11.24 nm and a PDI of 0.242 ± 0.041, indicating poor stability due to micelle formation. After 2 weeks, the globule size increased to 282.69 ± 12.41 nm with a PDI of 0.367 ± 0.078, reflecting some improvement.

In cases where larger globules were present during ultrasonication, they may break apart due to collapse, cavity formation, and microjet generation, allowing smaller, uniform globules to form as surfactants adsorb onto these new globules.[38] In formulations lacking sonication, the aqueous micellar solution leads to the dissolution of oil and micelle swelling, contributing to aggregation and decreased stability.[38] The zeta potential measured at −19.70 ± 0.052 mV for Opt-EUGE-NE11 also suggests stability for up to 14 weeks, likely

https://doi.org/10.1021/acsomega.5c00783
ACS Omega 2025, 10, 16815−16840

because of the presence of Tween-80, a nonionic surfactant that enhances stability.[66]

Overall, the stability study indicates that utilizing ultrasonic methods followed by chemical engineering strategies may be effective in extending the stability of nanoemulsions over a maximum period.

GC-MS/MS Study. Figure 15 presents various chromatograms: extracted-blank brain (A), extracted-blank-plasma (B), Eugenol brain-homogenate (C), and Eugenol plasma extraction (D). The recovery rate of Eugenol from plasma and brain homogenate exceeded 79.01%, demonstrating linearity in the concentration range (1.0−3000.0 ng·mL^{-1}), with a regression value (r^2) greater than 0.999. The method exhibited good selectivity, and the confirmation values for Eugenol in plasma and brain homogenate were all within acceptable limits, as indicated by the chromatograms. The coefficient of variation (%CV) for intra- and interbatch quality controls of Eugenol in both plasma and brain homogenate ranged from 1.10 to 1.86 and 1.6 to 2.10, respectively, while the accuracy percentages were between 98.02 to 99.83% for plasma and 90.91 to 99.66% for brain homogenate (Table 8). Stability results for Eugenol, detailed in Table 9, remained within acceptable limits across various storage conditions, including freeze−thaw cycles, long-term storage, postprocessing, and benchtop scenarios.[67]

PKs Parameters Examination. The trapezoidal method was employed to calculate pharmacokinetic (PK) parameters by plotting the concentration of Eugenol in the brain against time. The formulations EUGE-S, EUGE-NE, and CS-EUGE-NE were administered as a single dose via i.n. and i.v. routes, as illustrated in Figure 16 and Table 10. The maximum concentration (C_{max}) for EUGE-S was recorded at 79.61 ± 9.14 ng/mL (iv) and 111.52 ± 18.42 ng/mL (i.n.). In comparison, EUGE-NE reached C_{max} values of 193.64 ± 24.33 ng/mL (i.v.) and 1466.35 ± 33.64 ng/mL (i.n.). For CS-EUGE-NE, an elevated C_{max} of 289.73 ± 17.76 ng/mL (i.v.) and 1967.83 ± 49.69 ng/mL (i.n.) was observed, indicating significant differences (*p < 0.05, **p < 0.01, ***p < 0.001) (Table 10). Additionally, there was a notable increase in the intranasal area under the curve (AUC_{0-t}), with values of 1033.83 ± 44.24 ng·h/mg for EUGE-S, 23628.13 ± 96.79 ng·h/mg for EUGE-NE, and 2188.42 ± 73.69 ng·h/mg for CHS-EUGE-NE, also demonstrating significant variations (*p < 0.05, **p < 0.01, ***p < 0.001). The CHS-EUGE-NE formulation exhibited a maximum significant improvement when compared to EUGE-S (i.n.) due to its enhanced C_{max} and prolonged elimination rate. Our findings suggest that all formulations (EUGE-S, EUGE-NE, and CHS-EUGE-NE) displayed improved brain bioavailability when administered via the intranasal route compared to other administration methods. Finally, it was concluded that based on these results, the i.n.-route is the most effective method for delivering of Eugenol to the brain, a conclusion that has also been supported in prior studies.[38,42]

Pharmacodynamic Study in Depression. *Locomotor Activity Test (LAT).* A photoactometer was utilized to assess the locomotor activity of all preselected animal groups (Figure 17A). A photobeam was directed into the chamber to measure the locomotion of each animal over a period of 5 min. The results indicated that the locomotor activity patterns were consistent with those observed in the FST. The formulations CHS-EUGE-NE (p < 0.001) and EUGE-NE (p < 0.01) demonstrated significantly enhanced locomotor activity compared to the control groups. Furthermore, EUGE-S

Table 9. Validation: Stability Data for Eugenol (EUGE) in the Plasma and Brain Homogenates[a]

Exposure condition	LQC (2.92 ng/mL or ng g^{-1})		MQC (1250.00 ng/mL or ng g^{-1})		HQC (2400.00 ng/mL or ng g^{-1})	
	Brain Homogenate	Plasma	Brain Homogenate	Plasma	Brain Homogenate	Plasma
Long-Term Stability; Recovery (ng) after Storage (−80 °C)						
Previous day	2.92 ± 0.053	2.91 ± 0.055	1245.31 ± 20.14	1243.17 ± 19.34	2394.92 ± 44.32	2391.49 ± 41.63
30th Day	2.81 ± 0.047 (96.23%)	2.79 ± 0.049 (95.88%)	1231.61 ± 19.21 (98.90%)	1223.64 ± 20.19 (98.43%)	2366.79 ± 49.82 (98.83%)	2353.43 ± 40.12 (98.41%)
Freeze−Thaw Stress; Recovery (ng) after Freeze−Thaw Cycles (−80 to 25 °C)						
Pre-Cycle	2.91 ± 0.054	2.90 ± 0.049	1241.63 ± 21.48	1244.21 ± 19.64	2392.63 ± 41.64	2399.61±39.65
First Cycle	2.90 ± 0.052 (99.66%)	2.85 ± 0.047 (98.28%)	1222.49 ± 18.21 (98.46%)	1223.64 ± 17.22 (98.35%)	2356.31 ± 39.47 (98.48%)	2353.64 ± 40.14 (98.08%)
Second Cycle	2.82 ± 0.043 (96.91%)	2.79 ± 0.043 (96.21%)	1213.61 ± 15.66 (97.74)	1208.69 ± 19.07 (97.17%)	2344.19 ± 40.34 (97.98%)	2341.67 ± 38.25 (97.57%)
Third Cycle	2.79 ± 0.046 (95.88%)	2.72 ± 0.044 (93.79%)	1202.27 ± 19.27 (96.83%)	1200.12 ± 19.05 (96.46%)	2339.64 ± 41.36 (97.79)	2309.97 ± 39.01 (96.26%)
Benchtop Stability; Recovery (ng) at Room Temperature (25 °C)						
0 h	2.89 ± 0.044	2.91 ± 0.048	1245.38 ± 19.64	1243.97 ± 23.64	2396.27 ± 41.50	2391.61 ± 43.21
24 h	2.82 ± 0.043 (97.58%)	2.81 ± 0.044 (96.56%)	1227.91 ± 18.21 (98.60%)	1222.43 ± 21.86 (98.27%)	2388.24 ± 39.78 (99.66%)	2379.48 ± 41.94 (99.49%)
Postprocessing Stability; Recovery (ng) after Storage in Autosampler (4 °C)						
0 h	2.91 ± 0.045	2.90 ± 0.045	1241.82 ± 19.40	1242.00 ± 17.41	2392.75 ± 38.56	2387.36 ± 36.79
4 h	2.79 ± 0.043 (95.88%)	2.83 ± 0.041 (97.59%)	1219.64 ± 16.33 (98.21%)	1199.36 ± 18.56 (96.57%)	2371.64 ± 41.36 (99.12%)	2364.21 ± 39.64 (99.03%)

[a]Values (Mean ± SD) are derived from six replicates. Figures in parentheses represent analyte concentration (%) relative to time. Zero. Theoretical contents; LQC: 2.92 ng mL^{-1}; MQC: 1250.00 ng mL^{-1}; and HQC: 2400.00 ng mL^{-1}.

https://doi.org/10.1021/acsomega.5c00783
ACS Omega 2025, 10, 16815−16840

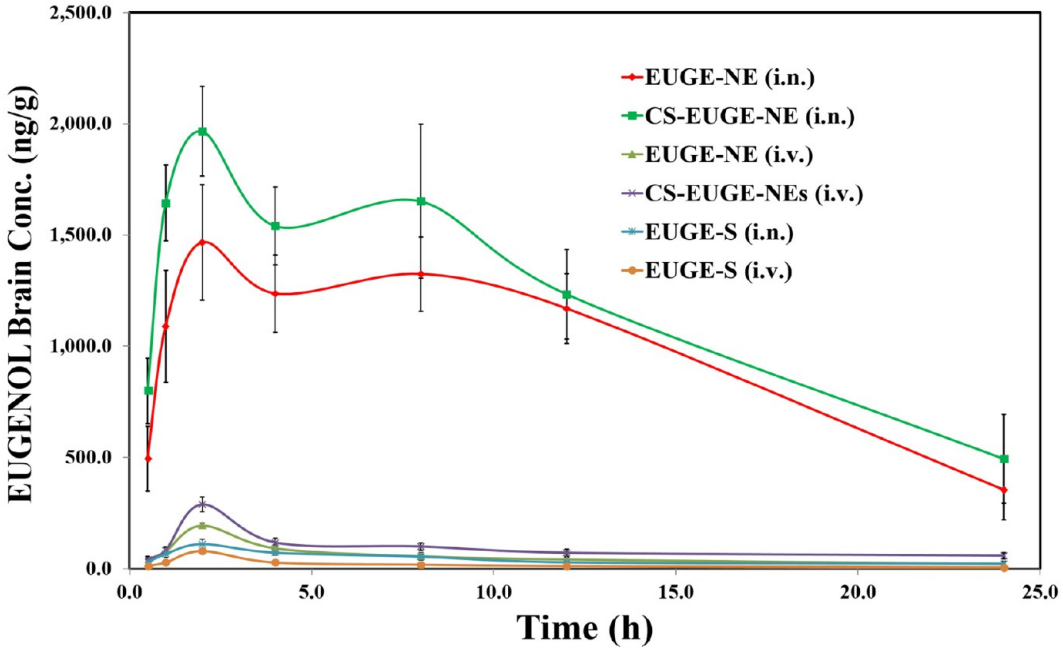

Figure 16. Pharmacokinetic profiles of Eugenol concentration in brain at various time intervals after given of optimized-CHS-EUGE-NE and optimized-EUGE -NE as compared with EUGE-S (pure).

Table 10. PK of Eugenol After I.N. and I.V. Administration to Rats at the Dose of 10 mg kg $^{-1}$ in Brain and Plasma (n = 6, Mean ± SD)

Formulation Administration	Samples	C_{max} (ng/mL g)	T_{max}	$t_{1/2}$ (h)	k_e (h^{-1})	AUC_{0-t} (ng min/ml g)
EUGE-S (i.n.)	Brain	111.52 ± 18.42	2.0	15.59 ± 3.49	0.04446 ± 0.0010	1033.83 ± 44.24
	Plasma	69.89 ± 4.17	0.5	8.97 ± 3.11	0.07731 ± 0.00061	359.69 ± 17.56
EUGE-S (i.v.)	Brain	79.61 ± 9.14	2.0	9.89 ± 1.02	0.07006 ± 0.00099	432.69 ± 23.47
	Plasma	1999.64 ± 121.24	0.5	4.71 ± 0.53	0.14721 ± 0.00025	8671.35 ± 66.34
EUGE-NE (i.n.)	Brain	1466.35 ± 33.64	2.0	19.90 ± 2.67	0.03483 ± 0.00026	23628.13 ± 96.79
	Plasma	56.33 ± 3.43	2.0	11.31 ± 0.73	0.06130 ± 0.00009	480.46 ± 19.67
CS- EUGE-NE (i.n.)	Brain	1967.83 ± 49.69	2.0	17.23 ± 4.01	0.04023 ± 0.00011	28453.71 ± 155.28
	Plasma	99.78 ± 8.29	2.0	10.77 ± 0.97	0.06435 ± 0.00011	1039.10 ± 75.09
EUGE-NE (i.v.)	Brain	193.64 ± 24.33	2.0	12.50 ± 2.11	0.05543 ± 0.00016	1316.65 ± 24.82
	Plasma	1436.36 ± 41.64	1.0	14.09 ± 1.03	0.04921 ± 0.00023	15590.64 ± 165.33
CS- EUGE-NE (i.v.)	Brain	289.73± 17.76	2.0	31.40 ± 4.02	0.02207 ± 0.00014	2188.42 ± 73.69
	Plasma	1924.31 ± 108.14	1.0	17.85 ± 1.09	0.03883 ± 0.00023	21536.02 ± 199.78
EUGE-S (i.n.)	Brain/Plasma	1.60	4.0	1.74	0.58	2.88
EUGE-S (i.v.)	Brain/Plasma	0.04	4.0	2.10	0.48	0.05
EUGE-NE (i.n.)	Brain/Plasma	26.03	1.0	1.76	0.57	49.18
EUGE-NE (i.v.)	Brain/Plasma	0.14	2.0	0.89	1.13	0.09
CS-EUGE-NE (i.n.)	Brain/Plasma	19.72	1.0	1.60	0.63	27.38
CS-EUGE-NE (i.v.)	Brain/Plasma	0.15	2.0	1.76	0.57	0.10

Comparative Bioavailability[a] ($AUC_{i.n.}/AUC_{i.v.}$) (%)

Formulations	EUGE-S	EUGE-NE	CS-EUGE-NE
Blood	4.14	3.08	4.83
Brain	238.93*	1794.56***	1300.19***

[a]Parameters are derived using mean ± SEM values of 6 different estimations.

exhibited a notable enhancement in locomotor-activity when administered through the i.n.-route in comparison to the control groups.

FST: Forced Swimming Test. As shown in Figure 17B, all recorded immobility values were significantly different from those of the control-group i.e., $p < 0.001$. The formulations CHS-EUGE-NE ($p < 0.001$), EUGE-NE ($p < 0.01$), and EUGE-S ($p < 0.05$) administered intranasally resulted in a notable decrement in immobility as compared to control-group.

Initially, at the 15 min mark, the rats displayed limited mobility; however, following the administration of the various EUGE formulations between the pretest and test periods, there was an observable increase in activity, indicating improved mobility. Enhanced climbing and swimming behaviors were noted with the i.n. application of CHS-EUGE-NE ($p < 0.001$) and EUGE-NE ($p < 0.01$) when compared to control-group.

https://doi.org/10.1021/acsomega.5c00783
ACS Omega 2025, 10, 16815−16840

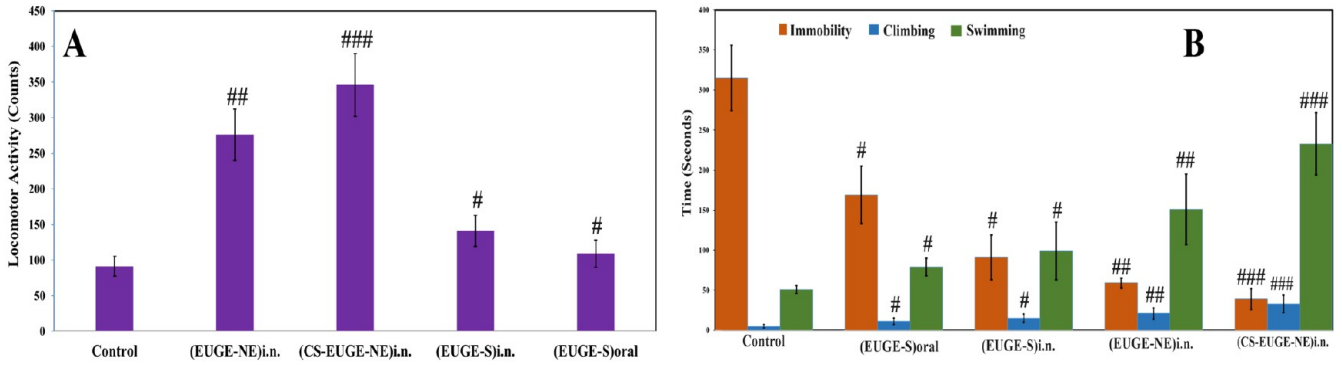

Figure 17. [A] Locomotor activity was performed for various types of formulations and their comparison with control groups and [B] evaluation of behavioral Forced swimming test (FST) for various types of formulations and their comparison with control groups.

Additionally, EUGE-S administered intranasally ($p < 0.05$) showed improvement in both climbing and swimming compared to the orally treated EUGE-S group after 24 h. These findings indicate a significant enhancement in the efficacy of the mucoadhesive-CHS-EUGE-NE formulation, attributed to its direct pathway to the brain, which facilitates outstanding brain-targeting along with sustained-release and enhanced permeation of Eugenol. The Forced Swimming Test (FST) was conducted to evaluate the potential effectiveness of various antidepressant drugs in rats. The results from the FST provided insights into the efficacy of these antidepressants for treating depression in humans.[53,68] FST is one of the most-widely utilized-methods for screening antidepressant-activity, recognized for its reliability and prevalence in academic research settings.[68]

Eugenol can extend its elimination time through controlled-release dosage forms, which contribute to prolonged retention and sustained physiological effects. Controlled-release formulations of Eugenol (EUGE) were developed, with EUGE-NE 5 being optimized after 20 trials for in vivo studies based on factors such as pH, drug content, ZP, globule-size, and viscosity (Tables 2 and 4). The Eugenol content was measured at 97.86 ± 0.38%. EUGE-NE 5 exhibited a pH ranging from 5.5 to 6.4, which is within the acceptable limits. It was characterized as a monodispersed and stable system with a globule size of 142.4 ± 5.36 nm and a PDI of 0.166 ± 0.0005, enabling effective delivery of Eugenol due to its large surface area. The zeta potential of EUGE-NE 5 was measured at −19.70 ± 2.31 mV, indicating significant physical stability ($p < 0.50$). Viscosity studies for EUGE-NE 5 supported its suitability for hassle-free administration during PK and pharmacodynamic examination.

The CHS-EUGE-NE formulation demonstrated a significant enhancement in brain bioavailability as compared to EUGE-S and EUGE-NE, marking a notable accomplishment for targeting the nose-to-brain pathway. CHS-EUGE-NE exhibited a prolonged residence time in the nasal cavity, attributed to chitosan with mucoadhesive properties. These properties facilitate the opening of tight junctions via positive charge interactions with the negatively charged cell-membrane surface, leading to enhanced-Eugenol permeability across the BBB and enabling controlled, sustained-drug-delivery. CHS has been utilized in numerous studies for intranasal targeting to the brain.[42,69] The encapsulation of drug was done in the NE that provided significant protection against biological and chemical degradation from the external environment, as well as facilitated extracellular transport through P-glycoprotein-mediated efflux. This mechanism contributes to the increased availability of the drug in CNS. The nanoscale of these formulations allows for easy transportation through olfactory-neurons to the brain, utilizing the olfactory-membrane's various endocytic-pathways found in sustentacular and neuronal cells, which is beneficial for treating diseases basically related to brain.[28] Based on the results of our research studies, CHS-EUGE-NE was employed to enhance the direct delivery of Eugenol (EUGE) to the brain, thereby improving its bioavailability and targeting.

Depression is a significant contributor to global suicide rates. Typically, treatments for depression are administered orally, which can lead to several side effects and limited therapeutic efficacy, resulting in patient intolerability. The antidepressant action of Eugenol relies on maintaining therapeutic concentrations in the central nervous system (CNS) over extended periods.[53] However, there are significant challenges in crossing the blood-brain barrier (BBB) when drugs are administered intravenously or orally. The intranasal route is considered the most effective for brain-targeted delivery, allowing drugs to reach the brain directly through neuronal and extracellular pathways. To enhance brain targeting via the intranasal route, we utilized chitosan, to create a mucoadhesive formulation of CHS-EUGE-NE.[42] The rat olfactory area, located in the posterior part of the nasal cavity, facilitates the delivery and absorption of drugs through this route. Therefore, the intranasal administration of drugs is an optimal strategy for treating brain disorders.[65] The mucoadhesive CHS-EUGE-NE formulation is a colloidal system designed to protect Eugenol from degradation during delivery through the intranasal route, enhancing its transport across mucosal barriers.[65]

Behavioral tests, including FST and LAT, were conducted to examine the effects of environmental changes. To minimize disturbances, all animals were transferred to their designated cages one h prior to testing, allowing them to acclimate to the testing environment. The pharmacodynamic (PD) studies demonstrated highly significant results for CHS-EUGE-NE when administered intranasally. Both CHS-EUGE-NE and EUGE-NE serve as lipid nanocarriers that notably enhance bioavailability of Eugenol (EUGE) to the brain via the nasal route compared to EUGE-S. Antidepressant action was improved with intranasal delivery due to the lipid characteristics of CHS-EUGE-NE and EUGE-NE.[42] Additionally, previous studies have reported that sodium taurocholate enhances permeability through the nasal mucosa, further supporting the effectiveness of CHS-EUGE-NE in delivering Eugenol for antidepressant effects.[70,71]

https://doi.org/10.1021/acsomega.5c00783
ACS Omega 2025, 10, 16815−16840

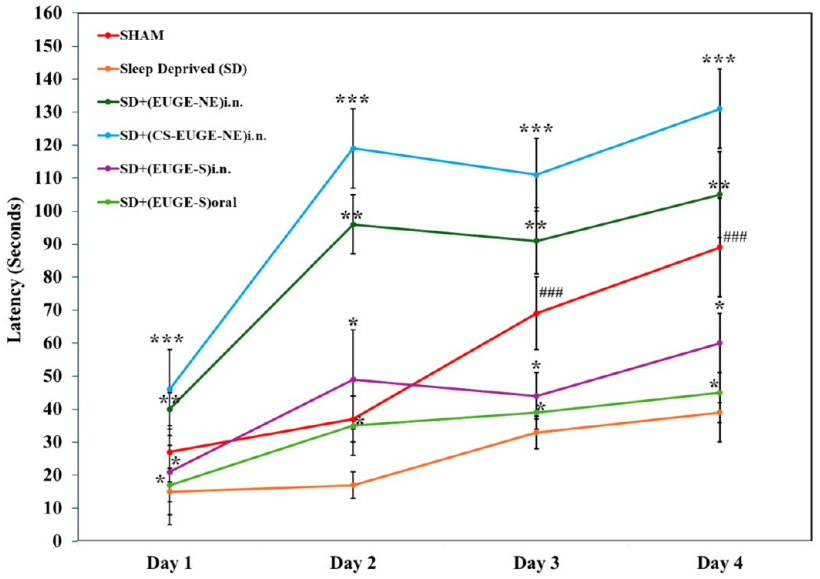

Figure 18. Motor learning in the rotor-rod test. The treatment with SD+(CHS-EUGE-NE)$_{i.n.}$ (*p < 0.0001), SD+(EUGE-NE)$_{i.n.}$ (*p < 0.001), SD +(EUGE-S)$_{i.n.}$ (*p < 0.01), SD+(EUGE-S)$_{oral}$ (*p < 0.01) as compared to sleep deprived (SD) for motor learning ability (starting 48 h post SD) across all 4-days learning SD.

The results indicated that EUGE-S administered orally led to only minimal improvement in behavior. Oral administration of Eugenol is hindered by factors such as acid hydrolysis and first-pass hepatic metabolism. Additionally, when administered via the oral route, Eugenol encounters challenges at the BBB. The drug's interaction with the BBB is limited due to the presence of efflux transporters, which restrict the delivery of various drugs to the brain.[53−55] Consequently, the intranasal route presents a promising alternative to increase bioavailability of drugs in the brain, as it minimizes metabolism and the effects of drug efflux at the BBB, which is less than initially expected.[55]

P-glycoprotein, a notable efflux transporter found in normal tissues, including intestinal epithelial cells and endothelial cells of the brain, plays a significant role in protecting and detoxifying the brain.[54] However, the substrate status of P-glycoprotein has not been well established in either in vitro or in vivo studies. Researchers are increasingly recognizing that the drug efflux mediated by ATP-binding cassette (ABC) transporters at the BBB can significantly limit the delivery of various therapeutics targeting brain disorders.[55] This limitation contributes to the challenges faced in treating many brain-related diseases.

We measured the levels of Eugenol in the brain to establish a connection between pharmacodynamics (PD) and pharmacokinetics (PK). The PD studies were conducted first, followed by the immediate removal of the brain for PK evaluation by using a GC-MS bioanalytical method. The administration of CHS-EUGE-NE resulted in a significantly greater concentration of Eugenol as compared to EUGE-S, demonstrating a strong linear correlation with the PD results (Figure 16). Intranasal delivery of CHS-EUGE-NE was notably more effective for therapeutic action than EUGE-S administered either intranasally or orally in treating depression.

During the forced swimming test (FST), we observed enhanced climbing and swimming behaviors associated with increased norepinephrine and serotonin levels. Additionally, improvements in neurotransmission were parallel to enhancements in locomotor activity as observed in the locomotor activity test (LAT).[9] Eugenol exhibited antidepressant effects when administered continuously over an extended period. The CHS-EUGE-NE formulation showed a delayed sustained release, leading to prolonged antidepressant effects.[8]

Both LAT and FST evaluations indicated the continuous presence of Eugenol in the synaptic cleft, resulting in a controlled release from the mucoadhesive nanoemulsion (CHS-EUGE-NE) compared to EUGE-S. Our treatment successfully improved the behavior of depressive rats using melatonin delivered via the mucoadhesive-Eugenol nanoemulsion i.e., CHS-EUGE-NE.[12] These findings indicate significant improvements in behavioral studies, such as locomotion and FST, in the depressive rats.

Rotor-Rod Test for Sleep. A significant effect on motor learning was observed during the 4 days of training, with notable differences between the groups. Furthermore, there was an important interaction between the group and the day of training. The results from Student's t-test indicated that the performance of the sleep-deprived (SD) group treated with the different formulations was significantly improved compared to the untreated SD rats on days 1 through 4 of the motor learning assessment. The most substantial improvement was noted on the fourth day, where the SD group receiving CHS-EUGE-NE via the intranasal route showed the greatest enhancement (*p < 0.0001), followed by the SD group receiving EUGE-NE, i.e., *p < 0.001, EUGE-S intranasally, i.e., *p < 0.01, and EUGE-S orally, i.e., *p < 0.01, all performing better than the standard SD group (Figure 18).

Toxicology Results. The toxicity assessment of CHS-EUGE-NE and CHS-NE (Placebo) administered via the intranasal (i.n.) route showed no mortalities across all groups during the 14-day period. No signs of irritation or tissue damage were observed in the nasal or brain tissues of rats treated with CHS-NE (Placebo). Macroscopic examination of both the nasal and brain tissues for CHS-EUGE-NE and CHS-NE revealed no alterations in the morphology or microstructure. CHS-EUGE-NE did not produce any visible signs of inflammation or necrosis when compared to the standard and normal control groups, confirming its safety (Figure 19). No

https://doi.org/10.1021/acsomega.5c00783
ACS Omega 2025, 10, 16815−16840

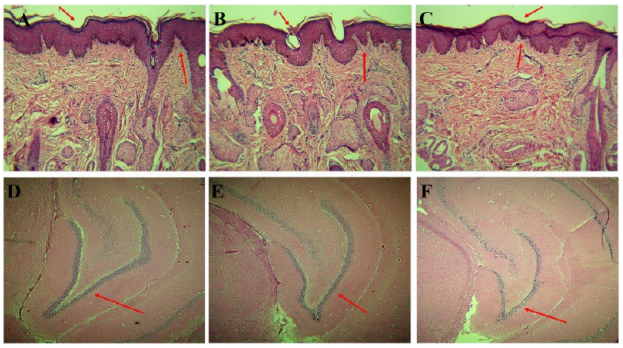

Figure 19. Photomicrographs represent the transverse section of A, B, and C images (nasal mucosa) and D, E, and F images (Rat's Brain) for normal control, CHS-NE (placebo), and CHS-EUGE-NE treated groups, respectively, after 14 days.

nasociliary damage was detected, and the nasal membrane remained intact following repeated treatments (Figure 19). The absence of visible signs of inflammation or necrosis indicates no toxicological effects. Therefore, all excipients used in this study were proven safe, and the toxicity results demonstrated the safety of CHS-EUGE-NE. Based on these results, CHS-EUGE-NE shows promise for future clinical and industrial applications. In this study, histopathological tissue examination was performed on brain and nasal mucosa samples collected from rats after 14 days of intranasal treatment with CHS-NE and CHS-EUGE-NE. The tissue samples were first fixed in 10% neutral-buffered formalin for 24 h to preserve cellular structure. After fixation, the samples were processed, embedded in paraffin, and sectioned into 5 μm thick slices. These sections were stained with eosin and hematoxylin (H&E) to evaluate general tissue morphology, cellular integrity, and any potential signs of inflammation or necrosis. The stained sections were examined under a light microscope to detect any histological changes. No pathological alterations such as inflammation, necrosis, or tissue damage were observed in the treated groups when compared to the normal control, confirming the safety of the formulation.

We found that the bioavailability of Eugenol in the brain was enhanced with CHS-EUGE-NE ($p < 0.01$) compared to EUGE-NE. Furthermore, CHS-EUGE-NE ($p < 0.01$) showed significant improvements in all pharmacodynamic parameters, including locomotor activity, immobility, climbing, swimming (FST), and sleep deprivation, compared to EUGE-NE.

CONCLUSION

BBD software was used to formulate EUGE-NE via ultrasonication, optimizing key parameters such as ultrasonication time, intensity, temperature, globule size, % transmittance, PDI, and zeta potential. The development of EUGE-NE involved the use of Clove Oil, a mixture of Tween-80 as a surfactant and PEG 400 as a cosurfactant. The Smix ratio of 3:1 was identified as optimal based on pseudoternary phase diagrams. Chitosan, a novel mucoadhesive polymer, was incorporated to create CHS-EUGE-NE, enhancing nasal mucosal permeability and prolonging residence time, thereby improving brain delivery while bypassing hepatic metabolism. TEM analysis confirmed smooth-surfaced globules under 200 nm. A validated GC-MS method was developed to evaluate pharmacokinetic parameters, revealing that intranasal CHS-EUGE-NE achieved higher C_{max} and brain bioavailability compared to EUGE-NE and EUGE-S. Behavioral studies in depressive rats demonstrated that CHS-EUGE-NE significantly improved swimming, climbing time, and locomotor activity while reducing immobility in the forced swimming test. Additionally, CHS-EUGE-NE enhanced motor learning in sleep-deprived rats. This optimized CHS-EUGE-NE formulation demonstrated safety and efficacy, supporting its potential for further clinical evaluation and future industrial application.

AUTHOR INFORMATION

Corresponding Authors

Niyaz Ahmad − *Department of Pharmaceutics, College of Dentistry and Pharmacy, Buraydah Colleges, Buraydah, Alqassim 51418, Saudi Arabia;* orcid.org/0000-0003-1874-6006; Phone: + 966 531203626; Email: niyazpharma@gmail.com, Niyaz.Husain@bpc.edu.sa

Mohd Faiyaz Khan − *Department of Clinical Pharmacy, College of Pharmacy, Prince Sattam bin Abdulaziz University, Alkharj 16278, Saudi Arabia*; Phone: + 966 502679269; Email: moh.khan@psau.edu.sa

Authors

Khalid Ansari − *Department of Respiratory Care, Faculty of Medical and Health Sciences, Liwa College, Abu Dhabi 41009, United Arab Emirates*

Zabih Ullah − *Department of Pharmaceutical Sciences, College of Dentistry and Pharmacy, Buraydah Colleges, Alqassim 51418, Saudi Arabia*

Hisham Osman Ibrahim − *Department of Respiratory Care, Faculty of Medical and Health Sciences, Liwa College, Abu Dhabi 41009, United Arab Emirates*

Hanan Mesfer Alyami − *Department of Medical and Surgical Nursing, College of Nursing, Princess Nourah Bint Abdulrahman University, Riyadh 13412, Saudi Arabia*

Ali Jaber Alqahtani − *Department of Emergency Medical Care, Faculty of Medical and Health Sciences, Liwa College, Abu Dhabi 41009, United Arab Emirates;* orcid.org/0000-0003-4934-2610

Sarfaraz Ahmad − *Department of Clinical Pharmacy, College of Pharmacy, Jazan University, Jazan 114, Saudi Arabia*

Complete contact information is available at: https://pubs.acs.org/10.1021/acsomega.5c00783

Author Contributions

[∞]Co-first authors: Mohd Faiyaz Khan and Niyaz Ahmad contributed equally.

Funding

This research was funded by Prince Sattam Bin Abdulaziz University, Project Number (PSAU/2023/03/25904).

Notes

The authors declare no competing financial interest.

ACKNOWLEDGMENTS

We sincerely thank Prince Sattam Bin Abdulaziz University for funding and supporting this research study.

REFERENCES

(1) Murray, C. J.; Lopez, A. D. Alternative projections of mortality and disability by cause 1990−2020: Global burden of disease study. *Lancet* **1997**, *349*, 1498−1504.

(2) Zeldetz, V.; Natanel, D.; Boyko, M.; Zlotnik, A.; Shiyntum, H. N.; Grinshpun, J.; Frank, D.; Kuts, R.; Brotfain, E.; Peiser, J. A new

method for inducing a depression-like behavior in rats. *J. Vis. Exp.* **2018**, *22*, 57137.
(3) Kessler, R. C.; McGonagle, K. A.; Zhao, S.; Nelson, C. B.; Hughes, M.; Eshleman, S.; Wittchen, H. U.; Kendler, K. S. Lifetime and 12-month prevalence of DSM-III-R psychiatric disorders in the United States. Results from the national comorbidity survey. *Arch. Gen. Psychiatry* **1994**, *51*, 8−19.
(4) Cryan, J. F.; Markou, A.; Lucki, I. Assessing antidepressant activity in rodents: Recent developments and future needs. *Trends Pharmacol. Sci.* **2002**, *23*, 238−245.
(5) Nestler, E. J.; Barrot, M.; DiLeone, R. J.; Eisch, A. J.; Gold, S. J.; Monteggia, L. M. Neurobiology of depression. *Neuron* **2002**, *34*, 13−25.
(6) Barden, N. Implication of the hypothalamic−pituitary−adrenal axis in the physiopathology of depression. *J. Psychiatry Neurosci.* **2004**, *29* (3), 185−193.
(7) Pramod, K.; Ansari, S. H.; Ali, J. Pramod Kannissery, Shahid H Ansari, Javed Ali. Eugenol: A natural compound with versatile pharmacological actions. *Nat. Prod. Commun.* **2010**, *5* (12), 1999−2006.
(8) Irie, Y.; Itokazu, N.; Anjiki, N.; Ishige, A.; Watanabe, K.; Keung, W. M. Eugenol exhibits antidepressant-like activity in mice and induces expression of metallothionein-III in the hippocampus. *Brain Res.* **2004**, *1011*, 243−246.
(9) Irie, Y. Effects of Eugenol on the Central Nervous System: Its Possible Application to Treatment of Alzheimer's Disease, Depression, and Parkinson's Disease. *Curr. Bioact. Compd.* **2006**, *2*, 57−66.
(10) Tao, G.; Irie, Y.; Li, D.-J.; Wing, M. K. Eugenol and its analogs inhibit monoamine oxidase A and exhibit antidepressant like activity. *Bioorg. Med. Chem.* **2005**, *13* (15), 4777−4788.
(11) Garabadu, D.; Shah, A.; Ahmad, A.; Joshi, V. B.; Saxena, B.; Palit, G.; Krishnamurthy, S. Eugenol as an anti-stress agent: Modulation of hypothalamic pituitary−adrenal axis and brain monoaminergic systems in a rat model of stress. *Stress* **2011**, *14* (2), 145−155.
(12) Müller, M.; Pape, H.-C.; Speckmann, E.-J.; Gorji, A. Effect of Eugenol on Spreading Depression and Epileptiform discharges in rat neocortical and hippocampal tissues. *Neuroscience* **2006**, *140*, 743−751.
(13) Oliveira, M. C.; Cavalcante, I. L.; de Araújo, A. N.; Ferreira dos Santos, A. M.; de Menezes, R. P.; Herrera-Acevedo, C.; Ferreira de Sousa, N.; de Souza Aquino, J.; Barbosa-Filho, J. M.; de Castro, R. D.; et al. Methyleugenol Has An Antidepressant Effect In a Neuroendocrine Model: In Silico And In Vivo Evidence. *Pharmaceuticals* **2023**, *16*, 1408.
(14) National Sleep Foundation. *2009 Sleep in America Poll*. www.sleepfoundation.org/sleep-pollsdata/sleep-in-america-poll/2009-health-and-safety, accessed 20 October 2014.
(15) Roth, T.; Coulouvrat, C.; Hajak, G.; et al. Prevalence and perceived health associated with insomnia based on DSMIV-TR; international statistical classification of diseases and related health problems, tenth revision; and research diagnostic Criteria/International classification of sleep disorders, second edition criteria: Results from the America Insomnia Survey. *Biol. Psychiatry* **2011**, *69*, 592−600.
(16) National Institutes of Health*Sleep disorders research plan*NIH Publication201111−7820
(17) Ferrie, J. E.; Kumari, M.; Salo, P.; et al. Sleep epidemiology—a rapidly growing field. *Int. J. Epidemiol.* **2011**, *40*, 1431−1437.
(18) Shahly, V.; Berglund, P.; Coulouvrat, C.; et al. The associations of insomnia with costly workplace accidents and errors: Results from the America Insomnia Survey. *Arch. Gen. Psychiatry* **2012**, *69*, 1054−1063.
(19) Kessler, R.; Berglund, P.; Coulouvrat, C.; et al. Insomnia and the performance of US workers: Results from the America Insomnia Survey. *Sleep* **2011**, *34*, 1161−1171.
(20) Sarsour, K.; Kalsekar, A.; Swindle, R.; et al. The association between insomnia severity and healthcare and productivity costs in a health plan sample. *Sleep* **2011**, *34*, 443−450.
(21) Rosekind, M. R.; Gregory, K. B. Insomnia risks and costs: Health, safety, and quality of life. *Am. J. Manag. Care* **2010**, *16*, 617−626.
(22) Lie, J. D.; Tu, K. N.; Shen, D. D.; Wong, B. M. Pharmacological Treatment of InsomniaPharmacological Treatment of Insomnia. *P&T* **2015**, *40* (11), 759−771.
(23) Benca, R. M.; Cirelli, C.; Tononi, G. Basic science of sleep. In *Kaplan and Sadock's Comprehensive Textbook of Psychiatry*, 9th, ed; Sadock, B. J.; Sadock, V. A.; Ruiz, P., Eds.; Lippincott Williams & Wilkins, Philadelphia, PA, 2009, pp. 362−375.
(24) Sahin, S.; Eulenburg, V.; Heinlein, A.; Villmann, C.; Pischetsrieder, M. Identification of eugenol as the major determinant of GABAA-receptor activation by aqueous Syzygium aromaticum L. (clove buds) extract. *J. Funct. Foods* **2017**, *37*, 641−649.
(25) Javahery, S.; Nekoubin, H.; Moradlu, A. H. Effect of anaesthesia with clove oil in fish (review). *Fish Physiol. Biochem.* **2012**, *38* (6), 1545−1552.
(26) Lee, M.-K.; Lim, S.; Song, J.-A.; Kim, M.-E.; Hur, M.-H. The effects of aromatherapy essential oil inhalation on stress, sleep quality and immunity in healthy adults: Randomized controlled trial. *Eur. J. Integr. Med.* **2017**, *12*, 79−86.
(27) Lawless, J. *The complete illustrated guide to aromatherapy: A practical approach to the use of essential oils for health and well-being*; HarperCollins UK, 1997.
(28) Ahmad, N. Rasagiline-encapsulated chitosan-coated PLGA nanoparticles targeted to the brain in the treatment of parkinson's disease. *J. Liq. Chromatogr. Relat. Technol.* **2017**, *40* (13), 677−690.
(29) Dhuria, S. V.; Hanson, L. R.; Frey, W. H. Intranasal delivery to the central nervous system: Mechanism and experimental consideration. *J. Pharm. Sci.* **2010**, *99*, 1654−1673.
(30) Pires, A.; Fortuna, A.; Alves, G.; et al. Intranasal drug delivery: How, why and what for. *J. Pharm. Sci.* **2009**, *12*, 288−311.
(31) Mittal, D.; Ali, A.; Md, S.; et al. Insights in to direct nose to brain delivery: Current status and future perspective. *Drug Delivery* **2014**, *21*, 75−86.
(32) Davis, S. S. Biomedical applications of nanotechnology − implications for drug targeting and gene therapy. *Trends Biotechnol.* **1997**, *15*, 217−224.
(33) Illum, L. Transport of drugs from the nasal cavity to central nervous system. *Eur. J. Pharm. Sci.* **2000**, *11*, 1−18.
(34) Qian, C.; McClements, D. J. Formation of nanoemulsions stabilized by model food-grade emulsifiers using high-pressure homogenization: Factors affecting particle size. *Food Hydrocolloids* **2011**, *25* (5), 1000−1008.
(35) Tadros, T.; Izquierdo, P.; Esquena, J.; Solans, C. Formation and stability of nanoemulsions. *Adv. Colloid Interface Sci.* **2004**, *108−109*, 303−318.
(36) McClements, D. J. Nanoemulsions versus microemulsions: Terminology, differences, and similarities. *Soft Matter* **2012**, *8*, 1719−1729.
(37) Sivakumar, M.; Tang, S. Y.; Tan, K. W. Cavitation technology—a greener processing technique for the generation of pharmaceutical nanoemulsions. *Ultrason. Sonochem.* **2014**, *21* (6), 2069−2083.
(38) Ahmad, N.; Khalid, M. S.; Al Ramadhan, A. M.; Alaradi, M. Z.; Al Hammad, M. R.; Ansari, K.; Alqurashi, Y. D.; Khan, M. F.; Albassam, A. A.; Ansari, M. J.; et al. Preparation of melatonin novel-mucoadhesive nanoemulsion used in the treatment of depression. *Polym. Bull.* **2023**, *80*, 8093−8132.
(39) Ahmad, N.; Ansari, K.; Alamoudi, M. K.; Ullah, Z.; Haque, A.; Ibrahim, H. O. Development of novel nanoemulsion of pioglitazone used in the treatment of diabetes and its gel form for the treatment of skin diseases. *J. Drug Delivery Sci. Technol.* **2024**, *100*, 106096.
(40) Ugwoke, M. I.; Agu, R. U.; Vanbilloen, H.; et al. Scintigraphic evaluation in rabbits of nasal drug delivery systems based on Carbopol 971 P and carboxymethylcellulose. *J. Controlled Release* **2000**, *68*, 207−214.
(41) Ahmad, N.; Ahmad, R.; Naqvi, A. A.; Alam, M.; Ashafaq, M.; Samim, M.; Iqbal, Z.; Ahmad, F. J. Rutin-encapsulated chitosan

https://doi.org/10.1021/acsomega.5c00783
ACS Omega 2025, 10, 16815−16840

nanoparticles targeted to the brain in the treatment of Cerebral Ischemia. *Int. J. Biol. Macromol.* **2016**, *91*, 640−655.
(42) Ahmad, N.; Rizwan, A.; Alam, M. A.; Samim, M.; Iqbal, J.; Ahmad, F. J. Quantification and evaluation of thymoquinone loaded mucoadhesive nanoemulsion for treatment of cerebral ischemia. *Int. J. Biol. Macromol.* **2016**, *88*, 320−332.
(43) Chang, S. F.; Huang, K. C.; Cheng, C. C.; Su, Y. P.; Lee, K. C.; Chen, C. N.; Chang, H. I. Glucose Adsorption to Chitosan Membranes Increases Proliferation of Human Chondrocyte via Mammalian Target of Rapamycin Complex 1 and Sterol Regulatory Element-Binding Protein-1 Signaling. *J. Cell. Physiol.* **2017**, *232*, 2741−2749.
(44) He, R.; Yin, C. Trimethyl Chitosan Based Conjugates for Oral and Intravenous Delivery of Paclitaxel. *Acta Biomater.* **2017**, *53*, 355−366.
(45) Chassary, P.; Vincent, T.; Guibal, E. Metal Anion Sorption on Chitosan and Derivative Materials: A Strategy for Polymer Modification and Optimum Use. *React. Funct. Polym.* **2004**, *60*, 137−149.
(46) Fernandez-Urrusuno, R.; Romani, D.; Calvo, D. Development of a freeze dried formulation of insulin-loaded chitosan nanoparticles intended for nasal administration. *STP Pharm. Sci.* **1999**, *9*, 429−436.
(47) Mayr, C. M.; Capone, D. L.; Pardon, K. H.; Black, C. A.; Pomeroy, D.; Francis, I. L. Quantitative Analysis by GC-MS/MS of 18 Aroma Compounds Related to Oxidative Off-Flavor in Wines. *J. Agric. Food Chem.* **2015**, *63* (13), 3394−3401.
(48) Zhao, X.; Wu, H.; Wei, J.; Yang, M. Quantification and characterization of volatile constituents in Myristica fragrans Houtt. by gas chromatography-mass spectrometry and gas chromatography quadrupole-time-of-flight mass spectrometry. *Ind. Crops Prod.* **2019**, *130*, 137−145.
(49) Das, A. K.; Sarkar, U. R.; Paul, P.; Hassan, M. J.; Banik, R.; Das, U. C.; Alam, M. K.; Islam, M. N.; Mahmud, M. H.; Shermily, N.; et al. Phytochemical Screening, GC-MS Analysis, and Evaluation of Antioxidants, Cytotoxicity, Analgesic, and Anti-Diarrheal Activity of the Extracts of the Leaves of Syzygium reticulatum Wight Walp. *Trends Sci.* **2024**, *21* (8), 7578.
(50) Anwer, M. K.; Aldawsari, M. F.; Iqbal, M.; Almutairy, B. K.; Soliman, G. A.; Aboudzadeh, M. A. Diosmin-Loaded Nanoemulsion-Based Gel Formulation: Development, Optimization,Wound Healing and Anti-Inflammatory Studies. *Gels* **2023**, *9*, 95.
(51) Ahmed, S.; Gull, A.; Alam, M.; Aqil, M.; Sultana, Y. Ultrasonically tailored, chemically engineered and "QbD" enabled fabrication of agomelatine nanoemulsion; optimization, characterization, ex-vivo permeation and stability study. *Ultrason. Sonochem.* **2018**, *41*, 213−226.
(52) Ahmad, N.; Ahmad, R.; Al-Qudaihi, A.; Alaseel, S. E.; Fita, I. Z.; Khalid, M. S.; Pottoo, F. H. Preparation of a novel curcumin nanoemulsion by ultrasonication and its comparative effects in wound healing and the treatment of inflammation. *RSC Adv.* **2019**, *9*, 20192−20206.
(53) Haque, S.; Md, S.; Sahni, J. K.; Ali, J.; Baboota, S. Development and evaluation of brain targeted intranasal alginate nanoparticles for treatment of depression. *J. Psychiatr. Res.* **2014**, *48*, 1−12.
(54) Pandey, Y. R.; Kumar, S.; Gupta, B. K.; Ali, J.; Baboota, S. Intranasal delivery of paroxetine nanoemulsion via the olfactory region for the management of depression: Formulation, behavioural and biochemical estimation. *Nanotechnology* **2016**, *27*, 025102.
(55) Alam, M. I.; Baboota, S.; Ahuja, A.; Ali, M.; Ali, J.; Sahni, J. K. Intranasal administration of nanostructured lipid carriers containing CNS acting drug: Pharmacodynamic studies and estimation in blood and brain. *J. Psychiatr. Res.* **2012**, *46* (9), 1133−1138.
(56) Ruiz-Vega, G.; Perez-Ordaz, L.; Leon-Hueramo, O.; Cruz-Vazquez, E.; Sanchez-Diaz, N. Comparative effect of Coffea cruda potencies on rats. *Homeopathy* **2002**, *91*, 80−84.
(57) Ruiz-Vega, G.; Poitevin, B.; Perez-Ordaz, L. Histamine at high dilution reduces spectral density in delta band in sleeping rats. *Homeopathy* **2005**, *94*, 86−91.
(58) Nunes, G. P., Jr.; Tufik, S.; Nobrega, J. N. Autoradiographic analysis of D1 and D2 dopaminergic receptors in rat brain after paradoxical sleep deprivation. *Brain Res. Bull.* **1994**, *34*, 453−456.
(59) Suchecki, D.; Lobo, L. L.; Hipolide, D. C.; Tufik, S. Increased ACTH and corticosterone secretion induced by different methods of paradoxical sleep deprivation. *J. Sleep Res.* **1998**, *7*, 276−281.
(60) Suchecki, D.; Tufik, S. Social stability attenuates the stress in the modified multiple platform method for paradoxical sleep deprivation in the rat. *Physiol. Behav.* **2000**, *68*, 309−316.
(61) Yang, R. H.; Wang, W. T.; Hou, X. H.; Hu, S. J.; Chen, J. Y. Ionic mechanisms of the effects of sleep deprivation on excitability in hippocampal pyramidal neurons. *Brain Res.* **2010**, *1343*, 135−142.
(62) Rechtschaffen, A.; Bergmann, B. M. Sleep deprivation in the rat: An update of the 1989 paper. *Sleep* **2002**, *25*, 18−24.
(63) Machado, R. B.; Suchecki, D.; Tufik, S. Comparison of the sleep pattern throughout a protocol of chronic sleep restriction induced by two methods of paradoxical sleep deprivation. *Brain Res. Bull.* **2006**, *70*, 213−220.
(64) Ahmad, N.; Albassam, A. A.; Khan, M. F.; Ullah, Z.; Buheazah, T. M.; AlHomoud, H. S.; Al-Nasif, H. A. A novel 5-Fluorocuracil multiple-nanoemulsion used for the enhancement of oral bioavailability in the treatment of colorectal cancer. *Saudi J. Biol. Sci.* **2022**, *29* (5), 3704−3716.
(65) Md, S.; Khan, R. A.; Mustafa, G.; Chuttani, K.; Baboota, S.; Sahni, J. K.; Ali, J. Bromocriptine loaded chitosan nanoparticles intended for direct nose to brain delivery: Pharmacodynamic, pharmacokinetic and scintigraphy study in mice model. *Eur. J. Pharm. Sci.* **2013**, *48* (3), 393−405.
(66) Ahmad, N.; Ansari, K.; Alamoudi, M. K.; Haque, A.; Ullah, Z.; Khalid, M. S.; Ahmad, S. A novel mucoadhesive paliperidone-nanoemulsion developed using the ultrasonication method in the treatment of schizophrenia. *RSC Adv.* **2024**, *14*, 23952−23972.
(67) US FDA. *Guidance for Industry Bioanalytical Method Validation*, 2001. http://www.fda.gov/downloads/Drugs/GuidanceComplianceRegulatoryInformation/Guidances/UCM070107.pdf. (Accessed 24 May 2018).
(68) Petit-Demouliere, B.; Chenu, F.; Bourin, M. Forced swimming test in mice: A review of antidepressant activity. *Psychopharmacology* **2005**, *177* (3), 245−255.
(69) Sani, I. K.; Geshlaghi, S. P.; Pirsa, S.; Asdagh, A. Composite film based on potato starch/apple peel pectin/ZrO2 nanoparticles/microencapsulated Zataria multiflora essential oil; investigation of physicochemical properties and use in quail meat packaging. *Food Hydrocolloids* **2021**, *117*, 106719.
(70) Mosmann, T. Rapid colorimetric assay for cellular growth and survival: Application to proliferation and cytotoxicity assays. *J. Immunol. Methods* **1983**, *65* (1−2), 55−63.
(71) Ahmad, N.; Al-Ghamdi, M. J. A.; Alnajjad, H. S. M.; Al Omar, B. B. A.; Khan, M. F.; Almalki, Z. S.; Albassam, A. A.; Ullah, Z.; Khalid, M. S.; Ashraf, K. A comparative brain Toxico-Pharmacokinetics study of a developed tannic acid nanoparticles in the treatment of epilepsy. *J. Drug Deliv. Sci. Technol.* **2022**, *76*, 103772.

https://doi.org/10.1021/acsomega.5c00783
ACS Omega 2025, 10, 16815−16840